Retour: TNO Defensie en Veiligheid, locatie Den Haag Postbus 96864, 2509 JG `s-Gravenhage

Infotheek TNO Defensie en Veiligheid, locatie Den Haag

Signatuur: R08-012 Computernr.: 123088

Exemplaar: 1

NUSP-2 02-09 KNMI-publicatie:200

# **Aerosol Retrieval and Assimilation (ARIA)**

Final Report

G.H.L. Verver, J.S. Henzing, G. de Leeuw, C. Robles-Gonzalez, P.F.J. van Velthoven





This report describes a project carried out in the framework of the National User Support Programme 2001-2005 (NUSP-2) under the responsibility of the Netherlands Agency for Aerospace Programmes (NIVR)

# **Aerosol Retrieval and Assimilation (ARIA)**

Final Report

G.H.L. Verver, J.S. Henzing, P.F.J. van Velthoven

Royal Netherlands Meteorological Institute (KNMI)

C. Robles-Gonzalez, G. de Leeuw

TNO Physics and Electronics Laboratory (TNO-FEL)

NUSP-2 report 02-09 NUSP-2 project 4.1/AP-12 KNMI-publicatie: 200 december 2002 isbn 90-369-2223-2





This report describes a project carried out in the framework of the National User Support Programme 2001-2005 (NUSP-2) under the responsibility of the Netherlands Agency for Aerospace Programmes (NIVR)

# **Content**

Executive Summary	
Abstract	
1.	Introduction
1.1	The problem
1.2	Objective of the project
1.3	Involvement of users
2.	Approach Phase 1
2.1	Introduction
2.2	Retrieval of aerosol properties
2.2.1	ATSR-2
2.2.2	AOS retrieval method
2.3	Aerosol modelling
2.4	Aerosol assimilation
3.	Results Phase 1
3.1	Introduction
3.2	Retrieval of aerosol properties
3.3	Aerosol modelling
3.3.1	Emission inventories-source
3.3.2	Wet and dry deposition-sink
3.4	Aerosol assimilation
4.	Conclusions
5.	Outlook to Phase 2

# Acknowledgements

# References

Appendix 1: The Advisory Group Appendix 2: Acronyms

# **Executive Summary**

Climate assessments are hampered by the large uncertainties involved in the estimation of the effect of atmospheric aerosol. These uncertainties are caused partly because sources and sinks as well as atmospheric processing of the different types of aerosol are not accurately known. Moreover, the climate impact (especially the indirect effect) of a certain aerosol distribution is hard to quantify. There have been different approaches to reduce these uncertainties. In recent years intensive observational campaigns like ACE and INDOEX have been carried out, aiming to increase our knowledge of atmospheric processes that determine the fate of atmospheric aerosol and to quantify the radiation effects. With the new satellite instruments, such as SCIAMACHY and OMI it will be possible in the near future to derive the geographical distribution of the aerosol optical depths (AOD) and perhaps additional information on the occurrence of different types of aerosol. With the assimilation of optical depth observations into an aerosol chemistry transport model it is in principle possible to obtain global 3-dimensional fields of aerosol, which are needed for the estimation of radiative forcing. Although the retrieval, assimilation, and aerosol modeling techniques are still under development, it is believed that the combination of satellite observations and modeling can lead to major improvements of the assessment of the effect of atmospheric aerosols on climate.

This report describes the work that has been done in phase 1 (from 15/9/2001 to 31/4/2002) of the project ARIA, Aerosol Retrieval and Assimilation. Partners in this project are KNMI and TNO-FEL. The project aims to improve the retrieval of aerosol optical depths from satellite instruments such as SCIAMACHY and OMI, and to develop an aerosol chemistry transport model as well as scheme for the assimilation of optical depth observations. Goal of phase 1 was to develop a working prototype of a complete retrieval-assimilation system.

#### Retrieval

The retrieval algorithm deals with the derivation of aerosol optical depths from radiances observed by a satellite instrument. The optical depth is a result of scattering and absorption of solar radiation by aerosol particles integrated over the whole atmospheric column. The algorithm therefore needs to make assumptions on the vertical distribution and the type of aerosol present in the column. There are several ways to obtain this information. In ARIA it was tried to extract aerosol type information from the spectral radiances observed by the ATSR-2 instrument. This method is based on the different wavelength dependences of the scattering and absorption of various aerosol types due to their chemical properties and particle size distributions. The following aerosol types were distinguished: dust, black carbon, and water soluble aerosols such as sea spray, ammonium sulphate, ammonium nitrate and hydrophilic carbonaceous aerosol. The method was tested over the Indian Ocean with data from the INDOEX campaign in 1999 (Ramanathan et al., 2001). Unfortunately in a first approach the algorithm was not able to distinguish between different aerosol mixtures without *a priori* information: the ground based data show the occurrence of five major aerosol types with similar weight. Because they fall roughly into two groups with similar spectral dependence it is not possible to discriminate between various mixing ratios. Another complication may be that the aerosol is not an external mixture (as is implicitly assumed by the algorithm) but an internal mixture.

In a second approach only a mixture was used of sea salt particles and an 'effective' aerosol type that was derived from sun photometer measurements on the Maldives during the INDOEX campaign (Dubovik et al., 2002). The aerosol optical depths (AOD) that were retrieved then showed good agreement with independent sun photometer data, i.e. AOD values agreed within 0.05 at 656nm. The AOD determined by the algorithm ranged from 0.4 over most over the continent to 0.1 in the Southern Hemispheric Indian Ocean. The aerosol mixing ration changed with fetch, i.e. the algorithm indicated the increasing sea salt contribution as the air mass was advected over the ocean. The method is only applicable to cloud free pixels. As part of the first phase of ARIA an automated cloud detection algorithm was implemented, based on Koelemeijer and Stammes (1999).

#### Model

The global three dimensional atmospheric chemistry transport model TM3 is used to calculate the distribution of atmospheric aerosol. This model already contained two aerosol types: sulphate and nitrate. In previous studies by Jeuken (2000) and Jeuken et al. (2001) it was shown that this is not sufficient to explain the optical depths observed by e.g. the ATSR-2 and GOME-instruments over Europe. Sometimes the contribution of the

aerosol types to the optical depth over Europe is less than 50 %. Therefore, as part of the ARIA project is was decided to implement additional aerosol types in TM3. In phase I organic and black carbon aerosols in hydrophobic and hydrophilic form were introduced based on Cooke (1999). The transformation rate of hydrophobic to hydrophilic carbonaceous aerosol is 0.87 day<sup>-1</sup>. In this phase of ARIA an extensive comparison of the model aerosol fields with observations was not feasible. Cooke (1999) estimated global scale emissions of carbonaceous aerosol from fossil fuel usage only. It is clear from literature that natural sources of carbonaceous aerosol as well as secondary production in the atmosphere are only very crude estimates (see Haywood and Boucher, 2000) for an overview). As a first rough estimate these two additional sources are accounted for by increasing the carbon aerosol emission from Cooke (1999) by a factor of 4.

#### Assimilation

Data assimilation as proposed in the ARIA project combines the model of atmospheric aerosol with optical depth values retrieved from satellite instruments. The satellite passes over a certain location of the Earth only at discrete times. The observations of the total column aerosol optical depth constrain the 3D modelled aerosol distribution at or around the location of the observation. The assimilation procedure developed in phase 1 is based on the scheme that is applied for the GOME total ozone observations (Eskes et al., 2002). This scheme was simplified by prescribing constant error covariances, instead of advecting the errors as is done in the original scheme. We choose to first gain insight in the analysis errors involved, before adding advection and growth of errors into the assimilation scheme. The parameter that is optimised is the 3 dimensional distribution of extinction coefficients due to the modelled aerosol types. The 3D distribution of aerosol mass of each type is subsequently adjusted by multiplication by a gain factor, which is the ratio of the analysed over the forecasted extinction coefficient.

The prototype assimilation system is applied for February 1999. The observations that were used are optical depths retrieved from the ATSR-2 instrument at 656nm over the INDOEX domain. The high resolution ATSR-2 data are averaged over each horizontal grid cell before being assimilated.

The prototype proved to be an efficient method for the integration of observations and model calculations. The impact of the observations on the results is large. The lifetime of the aerosol in the area is several days and the 24 hour forecasts of the AOD clearly improve by the assimilation. There is however a significant bias in the model, which systematically underestimates the optical depths when compared to the observations in the area. There are several explanations possible for this bias: (1) the natural emissions of carbon aerosol is too low, or incorrectly distributed over the globe, (2) dust and sea salt are not yet implemented in the model and (3) the optical properties of the modelled aerosols are highly uncertain and may not be correct.

#### Outlook to phase 2

Obviously the prototype needs a lot of improvements and extensive tests before it can serve as an operational system for the production of satellite retrieved aerosol data and of the global distribution of the main aerosol types. The quality of the AOD observations may be improved significantly when forecasted aerosol profiles of different types are used as a priori information for the retrieval algorithm. In phase 2 the source distribution of different types of aerosol in the model also needs to be refined, and additional aerosol types need to be implemented. The reason for the bias between observations and model forecast needs to be clarified. When the bias has been reduced the assimilation system can be evaluated, and parameters in the assimilation scheme itself can be updated. Moreover, it can be attempted to extract additional information on aerosol types from the spectral variation of observed optical depth. AOD retrieved from SCIAMACHY will be used instead of ATSR-2 data.

#### **ABSTRACT**

There are large uncertainties involved in the estimation of the effect of atmospheric aerosol on the climate. This is partly due to the crude representation of aerosols in global climate and chemistry models that are used to estimate the effects. Effective use of satellite instruments that observe atmospheric aerosol may lead to a major reduction of the uncertainty. The objective of the ARIA project is to derive from SCIAMACHY and OMI observations the geographical distribution of different types of aerosol as well as the aerosol optical depth. Goal of the first phase of the project was to develop a working prototype of a complete retrieval-assimilation system consisting of three modules: retrieval of the aerosol optical depth (AOD), global aerosol modelling and assimilation of the retrieved AOD. The INDOEX measurement campaign over the Indian Ocean in February and March, 1999, was used as a test case for the prototype system.

In the module to retrieve the aerosol optical depth assumptions must be made for the vertical distribution and the type of aerosol present in the column. This information can in principle be derived from the spectral dependence of the radiances observed by the satellite instrument. First results from the retrieval algorithm revealed that it was not feasible to derive a correct mixture of four basic aerosol types (water soluble aerosols, such as sulphate and nitrate; maritime aerosol; mineral dust; black carbon). In a second approach only a mixture was used of sea salt particles and an 'effective' aerosol type that was derived from sun photometer measurements on the Maldives during the INDOEX campaign (Dubovik et al., 2002). The aerosol optical depths that were retrieved then showed good agreement with independent sun photometer data, i.e. AOD values agreed within 0.05 at 656nm. The AOD determined by the algorithm ranged from 0.4 over most over the continent to 0.1 in the Southern Hemispheric Indian Ocean.

The global three dimensional atmospheric chemistry transport model TM3 was used to calculate the distribution of atmospheric aerosol (Jeuken,2000; Jeuken et al., 2001). As part of the ARIA project additional aerosol types were implemented in TM3, i.e. organic and black carbon aerosols in hydrophobic and hydrophilic form based on fossil fuel usage (Cooke, 1999). The transformation rate of hydrophobic to hydrophilic carbonaceous aerosol is 0.87 day<sup>-1</sup>. As a first rough estimate natural sources of carbonaceous aerosol as well as secondary production in the atmosphere are accounted for by increasing the carbon aerosol emission from Cooke (1999) by a factor of 4.

The procedure for the assimilation of satellite observed aerosol optical depths into the TM3 model is based on the scheme that was applied for the GOME total ozone observations (Eskes et al., 2002). This scheme was simplified by prescribing constant forecast and observation error covariances, instead of advecting the errors as is done in the original scheme. The parameter that is optimised is the 3 dimensional distribution of extinction coefficients. The 3D distribution of aerosol mass of each aerosol type is subsequently adjusted by multiplication by a gain factor, which is the ratio of the analysed over the forecasted extinction coefficient. The assimilation method yields a fast and computationally efficient module for the integration of satellite observations and model results. The impact of the observations on the results is large, mainly because of a bias in the model, which systematically underestimates the optical depths when compared to the observations in the area. There are several explanations possible for this bias: (1) the natural emissions of carbon aerosol is too low, or incorrectly distributed over the globe, (2) dust and sea salt are not yet implemented in the model and (3) the optical properties of the modelled aerosols are highly uncertain and may not be correct. Since the lifetime of the aerosol in the area is several days, the model is able to fill in the gaps between satellite overpasses and the 24 hour forecasts of the AOD clearly improve by the assimilation.

# 1. Introduction

# 1.1 The problem

One of the major challenges in climate research is the assessment of climate forcing by aerosols on global and regional scales. Aerosols scatter and absorb solar and infrared radiation. Depending on aerosol type this direct radiative forcing may be positive or negative. Aerosols also have an indirect effect on radiative forcing because they can act as cloud condensation nuclei and influence cloud albedo and lifetime. The latest estimate by IPCC (2001) of the direct radiative forcing by aerosols is  $-0.5 \text{ W/m}^2$ . Their indirect forcing is also negative and quite uncertain, between 0 and  $-2 \text{ W/m}^2$ . The radiative forcing by long-lived greenhouse gases is positive and quantitatively well known. The radiative forcing by the anthropogenic increase in greenhouse gases since 1750 is estimated at 2.43 W/m² by IPCC (2001). Hence, the total radiative forcing by anthropogenic aerosols is of the same order of magnitude as the forcing by the anthropogenic greenhouse gases, but of opposite sign and it has a much larger level of uncertainty.

# The global mean radiative forcing of the climate system for the year 2000, relative to 1750

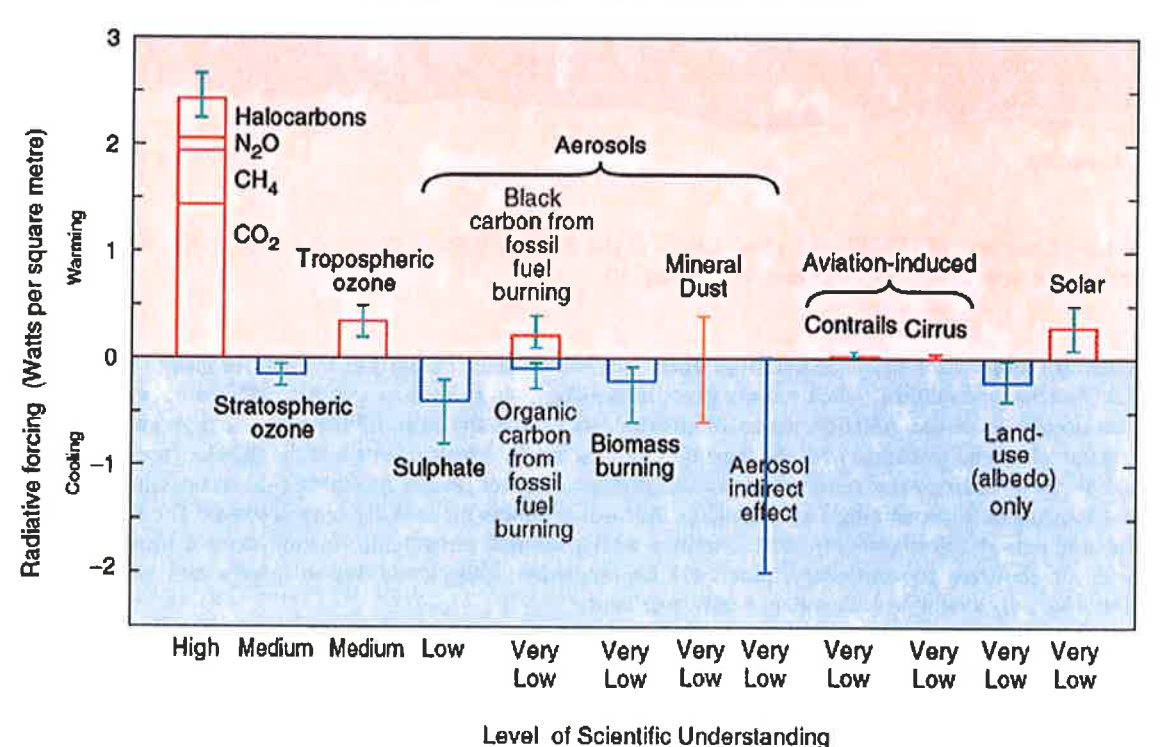


Figure 1.1 Radiative forcing of the climate system (IPCC, 2001)

Estimates of radiative forcing by aerosols in IPCC (2001) are mostly based on global transport models with simplified aerosol chemistry. Only very few observations exist that can be used to evaluate and improve such models. The most extensive observations have been made during recent international measurement campaigns such as ACE-1, ACE-2, TARFOX and INDOEX, where a variety of ground-based and airborne instruments were deployed. Results from these campaigns show large variations of aerosol properties with time and from one region to another. Therefore, results from these campaigns cannot be extrapolated to the

global scale. Global ground-based measurement networks, such as the sun-photometer network AERONET (Holben et al., 1998), provide only point measurements that are quite sparsely distributed over the globe (figure 1.2). A combination of global satellite observations and global modelling is the only alternative to understand the role of aerosols on climate forcing and to gain confidence in predictions about future climate change made with these models for climate assessments such as those coordinated by IPCC.



Figure 1.2: Locations of CIMEL sun photometers of the Aerosol Robotic Network (AERONET, Holben et al, 1998) in the year 2001 (http://aeronet.gsfc.nasa.gov).

Global aerosol information has been available since over two decades, but only as the aerosol index (AI) from the TOMS series of satellites which mainly gives information on absorbing aerosols, and the optical depth over the oceans from the AVHRR series of instruments. Since the mid 1990's more and more aerosol products have become available with the launching of new satellite instruments and the development of new retrieval algorithms. However, most of the aerosol products are not readily available since processing of the data is (yet) too time consuming (e.g., ATSR-2). Aerosol products are usually only retrieved for restricted areas and/or periods. Furthermore, most satellites with potential aerosol information do not have global coverage, i.e. they are geo-stationary, pixels are contaminated with clouds due to large swath widths, or algorithms are only available over water or only over land.

New instruments like OMI, and the recently launched SCIAMACHY, MODIS, and MISR are very promising. But even for this generation of satellite instruments a priori information is needed about the aerosol type and vertical distribution. This a priory information is sometimes based on measurements that are assumed to be representative for the region and the meteorological situation. Alternatively, a climatology of the distribution of various aerosol types and their vertical distribution has also been used as input. The latter operational approach is followed for the proposed OMI aerosol retrieval product, for which the algorithm is currently developed in a co-operation between KNMI and TNO-FEL, and NASA GSFC/University of Maryland for the AI. Such climatologies are also based on only a limited number of observations sparse in space and time.

The combined use of aerosol modelling and retrieval can lead to a major improvement because the effect of meteorological variability on aerosol concentrations is explicitly simulated. Also the growth of aerosols due to water uptake can be simulated using the modelled humidity. Aerosol modelling provides information on type and distribution of aerosol, and allows for the attribution of aerosol perturbations to specific sources. Aerosol densities from previous retrievals can be used in the aerosol chemistry-transport model through data assimilation (see below). The information on aerosol type and vertical distribution obtained from such a

model can be used in the retrieval algorithm to provide detailed information occurrence and frequency of specific aerosol types. In the ARIA project this technique is developed for application to SCIAMACHY and OMI data. The SCIAMACHY instrument was launched on ENVISAT on March 1, 2002; OMI is expected to be launched in January 2004. In the absence of SCIAMACHY during the first phase of ARIA, ATSR-2 data have been used to start the development of the methodology.

Whereas OMI provides data useful for aerosol retrieval only in the UV part of the spectrum, the wider spectrum from the UV to the near infrared of SCIAMACHY is an advantage for the retrieval of aerosol properties over sea because in the infrared the water surface is dark. Furthermore, the wider range of wavelengths allows for more accurate determination of the AOD wavelength dependence which in turn can be used to discriminate between various aerosol types, both over sea and over land. Aerosol retrieval results are available only during the satellite passes over cloud free areas. The assimilation of observations in an aerosol chemistry-transport model provides a means to fill in the gaps between subsequent retrievals, i.e. it yields the 4D distribution of aerosols in space and time.

Data assimilation is a technique that allows optimal use of observations of atmospheric compounds in a chemistry-transport model to derive global three-dimensional distributions of atmospheric species (e.g., Jeuken et al., 1999) The field of chemical data assimilation is in rapid development, however it is still strongly focussed on gaseous species, such as ozone. Recently, during the Indian Ocean experiment, a chemistry-transport model that assimilated aerosol optical thickness was applied (Collins et al., 2001). This was shown to be a promising approach for the evaluation of aerosol distributions and radiative forcing for the first time.

Up to five years ago aerosols were only crudely or not all represented in global climate and chemistry models. A WCRP workshop in 1995 revealed a variation by a factor of 3 in global annual mean sulphate burden between several global chemistry-transport models (Rasch et al., 1999). In recent years sophisticated parameterisations for various types of aerosols have been developed. A module for sulphate aerosol chemistry is now available for many models. It has long been thought that above industrialised regions, such as Europe and the USA, the aerosol optical depth is mainly determined by the ammonium salts of sulphate and nitrate. Recently, it was found that at northern mid-latitudes there may also be a relatively important contribution from other aerosol types (Jeuken et al., 2001; Ten Brink et al., 2001) such as organic aerosols (Russell et al.,1999; Robles-Gonzalez et al., 2001) and black carbon (Cooke et al., 1999). In the tropics and subtropics mineral dust and carbonaceous aerosols from biomass burning often constitute the dominant aerosol type. Few models yet contain all these different types of aerosol, although they have all been simulated in one model or another.

# 1.2 Objectives of the project

The primary objective of the ARIA project is the development of two aerosol products that can be derived from SCIAMACHY and OMI observations:

- the geographical distribution of aerosol optical depth constructed from retrieved aerosol data.
- the geographical distribution of aerosols obtained from assimilation of satellite observed optical depths in a 3D aerosol chemistry transport model.

Secondary objectives are:

- Improvement of retrieval algorithms for aerosol optical depth by using information in the infrared.
- Improvement of the retrieval by using information from an aerosol-chemistry model as input.
- Implementation of data assimilation of aerosol optical depths in an aerosol chemistry-transport model.
- Evaluation of the retrieval and assimilation products against independent observations.

The objectives and work involved in the project are divided into two phases.

#### Phase 1:

- Conversion of existing algorithms for application with SCIAMACHY. Extension of the retrieval algorithm to IR;
- Implementation of organic and black carbon aerosol in the chemistry-transport model TM3;
- Assimilation of single wavelength aerosol optical depths by proportional adjustment of the optical depths of the different aerosol types.

#### Phase 2:

- Implementation of the use of aerosol model output as a priori information for the retrieval of information on height and composition; evaluation and interpretation;
- Implementation of mineral dust aerosol in the chemistry-transport model TM3; evaluation by comparison with published results of other aerosol models and independent observations.
- Adapting the 1D assimilation scheme for multiple wavelength aerosol optical depths for use with TM3; evaluation of the improvement obtained by assimilating multiple wavelength observations.

This document reports on the work done in phase 1.

#### 1.3 Involvement of users

In the course of the project consultation of potential users of the new aerosol products took place, in order to ensure that the products will satisfy the different requirements. The use of the ARIA results is foreseen in several applications: i.e. the assessments of health risks in relation to human exposure to aerosols and UV radiation; the estimation of present day radiative forcing by aerosols (the direct effect); the attribution of climate change to different aerosol types and sources; the estimation of the indirect climate effect of aerosols; forecasting visibility for aircraft traffic and other applications.

A first consultation meeting of the ARIA advisory Group (AG), composed of 4 scientists employed in different working fields (see appendix 1), took place mid-November 2001. It was concluded that forecasts of aerosol concentration could be useful for the assessment of health risks caused by the exposure to air pollution and UV radiation. Although the direct result of ARIA are analysed fields of atmospheric aerosol, the tools needed to prepare forecasts are developed within the project.

The advisory group acknowledges the need for better estimates of the distribution of different aerosol types, as aimed for in this project, and better estimates of aerosol sources and sinks. The results of the first phase of the ARIA project were presented in several meetings:

- the General Assembly of the European Geophysical Society (EGS) in Nice, March 2002 (De Leeuw et al., 2002a; Verver et al., 2002);
- a workshop in chemical weather forecasting at DLR in Oberpfaffenhofen (Germany) in May 2002 (De Leeuw et al., 2002b);
- a workshop of ECMWF, in May 2002 in preparation of a extensive European initiative to monitor atmospheric composition using satellite instruments, including the assimilation of observations;
- the GAW workshop in Riga (Latvia) in May 2002 (De Leeuw et al., 2002c) where another extensive European initiative (AIROS) emerged to integrate ground-based observational networks (GAW and EMEP for gases and aerosols, EARLINET for lidars and PHOTONS for sun-photometers), satellite observations and models through 4D data assimilation, and
- the IWMMM conference in Steamboat (CO), USA (Robles-Gonzalez et al., 2002).

# 2. Approach for phase 1

#### 2.1 Introduction

To obtain a geographical distribution of aerosol optical depth and aerosol mass the observations retrieved from satellite instruments and model calculations are combined. A scheme of the system that has been implemented in phase 1 of the ARIA project, is depicted in figure 2.1.

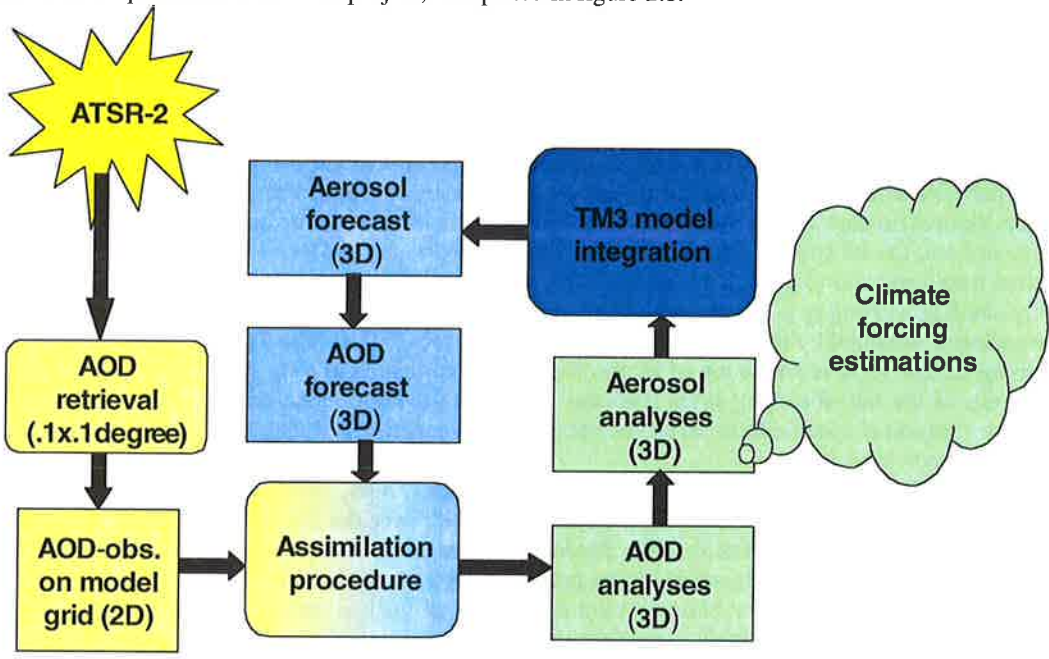


Figure 2.1 The aerosol retrieval and assimilation system as implemented in phase 1 of ARIA.

The first step in the assimilation system is the retrieval of aerosol optical depth from the observed ATSR-2 or SCIAMACHY radiances. The retrieval procedure is described in section 2.2 of this report. The observations are aggregated into 'super'observations, i.e. they are averaged over one grid cell which is then treated as one single observation. This reduces the computational costs considerably, which is a requirement when in the future much larger datasets with global coverage are assimilated. The TM3 model that is used to produce the aerosol forecast is described briefly in section 2.3. Section 2.4 describes the assimilation procedure itself

# 2.2 Retrieval of aerosol properties

Because in phase 1 of the ARIA project SCIAMACHY data were not available, aerosol properties were retrieved using ATSR-2 data. The existing algorithms for retrieval of aerosol optical depths developed for the ATSR-2 instruments have been extended to include more aerosol types. Also an automated cloud detection algorithm for application over land was developed, based on the work of Koelemeijer and Stammes (1999), to allow for the processing of large quantities of data.

The optical properties of aerosols are determined by their physical characteristics and chemical composition such as particle size distribution, particle shape and refractive index. The real part of the refractive index determines the scattering properties, the imaginary part determines the absorption. Aerosols such as sulphate or sea salt particles are not or little absorbing, in contrast to black carbon or desert dust aerosols which do absorb light. Aerosols of different origin and composition may also have a different size spectrum, and consequently a different wavelength dependence of the optical properties. To determine aerosol properties i.e.

the aerosol optical depth (AOD) from an optical signal such as the radiance at the top of the atmosphere (TOA), knowledge on the aerosol optical properties as function of wavelength is required. This information is provided by calculations of the aerosol scattering phase function, i.e. the intensity of the scattered light as function of the scattering angle, for the observed wavelengths. The expected TOA signal is then simulated using radiative transfer model. To reduce the processing time, look-up tables (LUT) are prepared with the calculated TOA radiances for different aerosol types and mixtures, at different wavelengths and for a series of satellite-sun geometry's.

The AOD and the wavelength dependence can be retrieved both over land and over water. The wavelength dependence of the AOD is described by the Ångström coefficient. Together, the AOD and the Ångström coefficient can be used to estimate the column integrated effective particle size distribution. The AOD provides information on the total aerosol burden in a certain size range; the Ångström coefficient gives an indication on the shape of the particle size distribution. Small values of the Ångström coefficient indicate the dominance of large particles, such as sea salt or dust, and large Ångström coefficients are usually obtained when small particles dominate, such as sulphates, ammonium nitrate, or biomass burning aerosol.

The aerosol mixture that is found at a certain location is a result of the distribution of sources and sinks of the aerosol, the subsequent advection and vertical transport, and processes leading to their chemical and physical transformation (e.g., Sokolik et al., 1998) due to various processes. In particular changes are induced by cloud processing (e.g., Raes et al., 2000). The vertical distribution of the aerosol layers will also affect the radiance measured by the satellite at the top of atmosphere (TOA). The TOA radiance is larger if a non-absorbing aerosol layer is on the top of an absorbing layer, compared to a situation where the absorbing layer is on top of the non-absorbing layer [Quijano et al., 2000]. Information on the composition of the aerosol mixture present at specific location can be obtained from experimental data, climatological data bases or chemistry transport models.

The ATSR-2 algorithms developed by Veefkind (Veefkind and de Leeuw, 1998, and Veefkind et al., 1998) consider only sea spray and continental aerosols. This works well over the US East coast (Veefkind et al., 1998) and western Europe (Veefkind et al, 2000; Robles Gonzalez et al., 2000) for which the algorithms were developed. However, to make the algorithms more generally applicable, also other aerosol types need to be accounted for, such as dust, soot or biomass burning aerosol as well as mixtures of aerosol types. The extension of the ATSR-2 dual and single view algorithms with such aerosol types was undertaken as part of the ARIA project. This is not straightforward because the overall effect of the mixture is not simply obtained by adding the effects of each type of aerosol that make up the mixture for reasons given above.

The goal of this work was to extend the ATSR-2 algorithms for more general application. The algorithms were tested with data obtained during the INDOEX experiment in 1999. A set of look up tables (LUT) was created based on aerosol measurements over the Indian Ocean and elsewhere. The new LUT's were used to retrieve the AOD over the Maldives area where an AERONET sun photometer [Holben et al., 1998] is placed. From the comparison with the sun photometer the two aerosol mixtures that best describe the AOD spectral dependence over the area have been selected. In ARIA phase 1 the algorithms have been developed and partly tested with data from the February 1999 INDOEX data. The limited time did not allow for the processing of the full INDOEX 1999 data. Results will be presented.

#### 2.2.1 ATSR-2

The ATSR-2 on board the European Remote Sensing Satellite ERS-2 is a radiometer with seven wavelength bands, four of which are in the visible and near-infrared parts of the spectrum (effective wavelengths 0.555, 0.659, 0.865 and 1.6  $\mu m$ ). The ATSR-2 has a conical scanning mechanism providing two views of each location: first a forward view (viewing zenith angle approximately 56°) and about two minutes later a nadir view. The spatial resolution is approximately 1x1 km² at nadir. The swath width of the ATSR-2 is 512 km. For the mid-latitudes, this results in an overpass over a given location once every three days.

New algorithms have been developed to retrieve the Aerosol Optical Depth (AOD) from ATSR-2 data based on the single view algorithm for application over sea (Veefkind and de Leeuw, 1998) and on the dual view algorithm for application over land (Veefkind et al., 1998). The single view algorithm assumes that the sea surface reflectance is low and constant. The dual view algorithm assumes that the ratio of the nadir and forward view of the ATSR-2 is independent of the wavelength (Flowerdew and Haigh, 1995). Additionally, it is assumed that the contribution of the aerosols is relatively small for the 1.6 µm channel.

These algorithms are based on a simple aerosol model describing the vertical distribution of an aerosol mixture consisting of continental aerosols and seaspray. The modelled aerosol reflectance as a function of the wavelength and the sun-satellite geometry is contained in look up tables (LUT's).

Aerosol optical properties can only be retrieved over cloud free areas. The cloud flag in the ATSR-2 data works properly over sea but over land it is too strict and selects high reflectance surfaces as cloudy. For the application of the dual view algorithm over Europe (Robles Gonzalez et al., 2000) the semi-automatic algorithm for cloud screening over land developed by Koelemeijer and Stammes (1999) was applied. The use of this algorithm for larger data sets is very time consuming. For instance, the detection of clouds for August 1997 (Robles-Gonzalez et al., 2000) with the semi-automatic scheme took two weeks. Therefore, for the application to large data sets an automated cloud detection algorithm was developed still based on the method of Koelemeijer and Stammes, 1999. Over land the algorithm uses differences in the brightness temperature and reflectance of clouds and land.

## 2.2.2 AOD retrieval method

To retrieve the AOD, the reflectance measured by the ATSR-2 radiometer is first corrected for atmospheric effects (i.e. absorption and scattering by molecules) and for surface effects. Then the corrected reflectance is compared with the pre-computed reflectance from look up tables (LUT) in order to know which aerosol type fits best the spectral reflectance of the aerosols present in the atmospheric column. For each aerosol type or mixture a LUT has to be computed. The scattering properties of the aerosol mixtures are calculated using a Mie program. Size distributions based on the OPAC aerosol model (Hess et al., 1998) are used to complete the information needed. The LUT's were created with the DAK (Doubling and Adding method) radiative transfer model (Stammes et al., 1989).

Two types of LUT's were considered, one based on single aerosol components (e.g. dust, sulphate, etc.), and one based on aerosol mixtures.

### Single component method

Aerosol mixtures in the atmosphere are created as combination of different aerosol components such as black carbon, water-soluble (sulphate, nitrate, some organic), sea salt and dust particles. Different aerosol mixtures are found around the Earth depending on local sources, sinks and transport processes. The optical properties of the aerosol mixtures depend on the percentage of every component included in the mixture and on the meteorological conditions such as relative humidity and vertical structure. In this part of our study, aerosols have been classified in 4 general types based on their chemical composition (Hess et al., 1998):

- 1.- water soluble aerosols (sulphate, nitrate, some types of organic aerosols, etc) which are non or little absorbing and of medium size,
- 2.- maritime aerosols, which are also little absorbing and have a bi-modal size distribution,
- 3.- dust, for which the absorbing capacity depends on their composition (Sokolik, 1998) and which has a bi-modal size distribution, and
- 4.- black carbon which is highly absorbing and of medium size.

A LUT for each of these aerosol components was made. The goal was to obtain information on the aerosol composition based on the satellite data. However, the algorithm was not able to detect the proper mixture using combinations of LUT's for the single components listed above. There may be several reasons for this. One of the difficulties using this method is that aerosols in nature may be internally mixed while the algorithm assumes external mixtures. Another reason may be the fact that, for instance, soluble particles and black carbon show similar spectral behaviour and the algorithm is not able to distinguish between them. Sea salt aerosol and dust particles also have similar spectral behaviours.

Therefore an alternative approach was followed in which LUT's were created using representative mixtures for the study area to retrieve the AOD for the same area. When no information is available on the aerosol composition, the aerosol mixtures can be obtained from climatologies. Possibly, a better initial estimate can be obtained from the application of chemical transport models with proper initialisation for the aerosol composition and concentrations, such as proposed for ARIA phase 2. An initialisation could be obtained from a scheme as described in Figure 2.1. In the current ARIA phase 1 the starting point has been the

measurements of the aerosol characteristics done during the INDOEX experiment presented in Quinn et al. (2001), Chowdhury et al. (2001), and Dubovik et al. (2002).

#### Method based on measurements

Data from the INDOEX campaign are available from various sources. Quinn et al., 2001, used a nephelometer and particle sizers on board the RV Ronald H. Brown to determine the composition and the optical properties of eight air masses with different source regions. For our application in the ATSR-2 algorithms only the Northern Hemispheric Indian Ocean (NHIO) aerosol type was used. Chowdhury et al., 2001, used cascade impactors to determine the chemical composition of the aerosols at the Kaashidhoo Climate Observatory (KCO) (Maldives), February 11-26, 1999. Dubovik et al., 2002, retrieved optical information of the aerosols using CIMEL ground-based radiometers from the AERONET data base (Holben et al., 1998). LUT's have been prepared based on each of these results and retrievals were made using ATSR-2 data obtained over the Maldives. The results were compared with the sunphotometer data at Male island. Based on this comparison, two aerosol types were selected for further processing, the KCO aerosol type measured at the Maldives Island and sea salt (obtained from the AERONET measurements at Hawaii).

# 2.3 Aerosol modelling

The model used to simulate aerosol distributions is TM3, a global three dimensional atmospheric chemistry transport model (Dentener et al., 1998, Meijer et al., 1999). This Eulerian model solves the tracer continuity equation on a regular latitude x longitude grid (10°x7.5°, 5°x3.75° or 2.5°x2.5°) and hybrid sigma-pressure coordinates in the vertical (31 layers). The tracer transport component in TM3 has been adapted from the global tracer transport model TM2 (Heimann, 1995). TM3 uses 6-hourly archived meteorological output of the weather forecast model of ECMWF (European Centre for Medium-range Weather Forecasts) to simulate atmospheric transport, thermodynamical properties such as temperature and humidity, and the distribution of clouds (Van Velthoven and Kelder, 1996). In a preprocessing step the meteorological fields are interpolated to the TM3 grid and wind fields are converted into air-mass fluxes through the sides of the TM3 grid boxes. The actual advection of tracers is done using the slopes scheme described by Russell and Lerner (1981). The TM3 model contains parameterisations for turbulent mixing, convective transport, and dry and wet deposition all based on the ECMWF parameters.

It includes a tropospheric chemistry scheme based on CBM-IV (Houweling et al., 1998). Sulphate, ammonium and nitrate aerosol chemistry has been added and evaluated by Jeuken (2000) in the framework of the national NOP-project Aerosol (Ten Brink et al., 2001). The TM3 model has been used to contribute to recent climate assessments by the IPCC, such as the Special Report on Aviation and the Global Atmosphere (1999) and the IPCC Third Assessment Report (IPCC-TAR, 2001).

As was shown by Jeuken (2000) and Jeuken et al. (2001) the inclusion of additional aerosol types will be necessary to explain the optical depths observed by e.g. the ATSR-2 and GOME-instruments over Europe. The presently included sulphate-ammonium-nitrate types sometimes explain less than 50 % of the optical depth over Europe. Therefore, in ARIA it was planned to extend TM3 with parameterisations of the most important aerosol types that were missing. In phase I of ARIA TM3 has been extended with organic and black carbon aerosols in hydrophobic and hydrophylic form, as described in 3.3. In total it now contains 26 tracers (including 6 aerosol species) involved in 100 chemical reactions causing tracer gains and losses.

# 2.4 Aerosol assimilation

Retrieval products from satellite instruments such as described in section 2.2 consist of data that is irregularly distributed in space and time. This is because the satellite passes over a certain location on earth only at discrete times. In addition retrievals are restricted to cloud-free situations.

The aerosol optical depth (AOD) can be derived from several satellite instruments such as SCIAMACHY, AVHRR and ATSR. Data assimilation allows the calculation of continuous fields in space and time from observations that are irregularly distributed (Jeuken et al., 1999). Moreover, the aerosol optical depth may provide information on sources, sinks and transport of different aerosol types that dominate the extinction (Collins et al., 2001; Rasch et al., 2001). Data assimilation is therefore expected to become a powerful tool to reduce the uncertainties in the estimation of the global and regional aerosol distribution.

The observations of the total column optical depth can be used to constrain of the modelled aerosol distribution at or around the time and location of the observation. The assimilation procedure yields an optimal estimation of the 4-dimensional (time and space) distribution of the extinction coefficients due to the presence of different types of aerosol. This optimum estimate accounts for assumed error distributions of both the model and the observations.

The parameter that is analysed is the aerosol optical depth by all aerosols in a grid cell in layer k,  $\tau_k$  (i.e. the product of the extinction coefficient and the depth of layer k). The total aerosol optical depth,  $\tau$ , is given by the sum over the aerosol optical depths in all K model layers:

$$\tau = \sum_{k=1}^{K} \tau_k \,, \tag{2.1}$$

where the optical depth of model layer k is given by:

$$\tau_{k} = g^{-1} \int_{p_{k}}^{p_{k+1}} \sum_{i} \chi_{i}(p) q_{i}(p) dp.$$
 (2.2)

Here i is an index looping over the aerosol species.  $\chi_i$  is the mass extinction coefficient for species i,  $q_i$  is the corresponding aerosol mass mixing ratio (kg aerosol / kg air), g is the gravitational acceleration, and  $p_k$  is the pressure at the lower boundary of layer k.

The assimilation of AOD requires the optical extinction coefficients  $\chi_i$  for each of the aerosol species. By prescibing  $\chi_i$  assumptions are implicitly made for each species about its size distribution and the light scattering and absorbtion properties. Sulfate optics are taken from Kiehl et al. (2000) including their extinction correction for hygroscopic growth. For dry sulfate aerosol they assumed a lognormal size distribution, with as parameters the mean radius  $r_g = 0.05 \, \mu m$  and the standard deviation  $\sigma_g = 2.03 \, \mu m$ , in accordance with d'Almeida et al.(1991). Humidification is then taken into account by growing the particles to a radius in equilibrium with the surrounding relative humidity using the Köhler equation (e.g. Seinfeld and Pandis, 1997). In Kiehl et al. (2000) the refractive index of sulfate is taken from Palmer and Williams (1975) and Gosse et al. (1997). Mie theory finally provides the effective sulfate optics of the two-component system of water and sulfate .

The mass extinction coefficients mentioned in the literature for carbonaceous aerosols vary from 2.5 to 12 m<sup>2</sup>/g, depending on the chemical and physical properties of this aerosol (Liousse et al., 1996; Tegen et al., 1997). We have implemented  $\chi_{Carbon} = 9$  m<sup>2</sup>/g for both hydrophobic and hydrophilic carbon following Haywood and Ramaswamy (1998). Since the uncertainties in  $\chi_{Carbon}$  for the dry carbon are much larger than in the typical hygroscopic growth factors, no hygroscopic growth is applied to the  $\chi_{Carbon}$ .

The assimilation procedure used in phase 1 of ARIA is based on the scheme that is applied for the GOME total ozone observations (Eskes et al., 2002) in the global chemistry / transport model TM3. The assimilation of total ozone observations is similar to the assimilation of aerosol optical depths. In both cases the observations are column integrals (total ozone / aerosol optical depth), while the parameter that is optimised (analysed) has a 3D distribution (ozone mass / aerosol optical depth per layer / gridpoint). The use of TM3 in both cases makes the implementation more straightforward.

However, there are also important differences between the AOD and total ozone. The lifetime of aerosol particles is much shorter: one to ten days (Tegen et al., 1997) as compared to an average of several weeks for

ozone in the lowermost stratosphere. The aerosol is predominantly present in the boundary layer and lower troposphere, while atmospheric ozone resides mainly in the stratosphere. Sources (emissions) and sinks (in particular wet deposition) of aerosols are very inhomogeneously distributed over the globe. As a consequence the variations of the AOD will have shorter length- and timescales than those of ozone. Moreover, the optical properties, the source strengths and atmospheric lifetimes of the different types of aerosol are often not well constrained.

These uncertainties in the aerosol properties have a strong impact on the behaviour and performance of the assimilation scheme. The determination of the assimilation parameters and the sensitivity of the system performance for these parameters will be the subject of future research.

The assimilation equation reads:

$$\tau_{k}^{a} = \tau_{k}^{f} + PH^{T} (HPH^{T} + R)^{-1} (\tau^{o} - H^{T} \tau_{k}^{f})$$
 (2.3)

where  $\tau_k^a$  and  $\tau_k^f$  are the modelled 3D distributions of the grid cell aerosol optical depth, the analysis and the forecast respectively;  $\tau^0$  is the AOD observation averaged over a TM3 cell (the aggregated or 'super'-observation); H is the observation operator; R is the observation error covariance matrix, and P is the forecast error covariance matrix.

The observation operator H is a simple matrix representing the sum over the vertical layers (equation 2.1). The use of aggregated observations avoids the spatial interpolation of model values to the location of the individual pixels. The size of the observation vector  $\tau^0$  is greatly reduced, since one ATSR-2 pixel is only 0.1° by 0.1°, while the horizontal model grid of TM3 is presently 2.5° x 2.5° (fine) or 10° x 7.5° (coarse). In this pilot study we used the coarse resolution.

The error covariance matrices determine the relative weighting of the model forecast and of the observations. Large forecast errors (P) and relative small observational errors (R) will result in a stronger adjustment towards the observations. When the observational data are highly uncertain, or when it is known that they are not representative for the grid cell, the associated large values in R will result in a small impact of the observations on the analyses.

The implemented scheme is an optimum interpolation assimilation scheme, i.e. the error covariance matrices are prescribed and kept constant in time. For the observations we defined a diagonal error covariance matrix R, implying that the observational errors are uncorrelated in space. We assume an observation error variance of 0.01, corresponding to an error in  $\tau^0$  of 0.1. We have chosen not to implement the advection and growth of the forecast error covariances (P) yet as in the GOME assimilation procedure.

The forecast error covariance between grid cell i and j is prescribed by (Eskes et al., 2002):

$$P_{ij} = \sigma_{\tau}^{2} \cdot f_{\text{vert}} \cdot f_{\text{hor}} \quad , \tag{2.4}$$

where we set the forecast error variance in the total optical depth  $\sigma_{\tau}^2$  equal to the observation error variance: i.e. 0.01, corresponding to a forecast error in  $\tau$  of 0.1.. Note that the prescribed values for the forecast error and the observation error will be updated after an examination of the error statistics and a comparison with independent observations. The vertical distribution of the error is done by the function  $f_{\text{vert}}$  that scales the error variance with the vertical distribution of  $\tau_k$ . The horizontal forecast error correlation is represented by the function  $f_{\text{hor}}$ , which scales the covariance with distance between grid cells i and j divided by a length scale L. In the current version of the assimilation module the horizontal correlation length scale L was set to 500 km (roughly  $5^{\circ}$  near the equator)

Finally, when equation (2.3) is solved and an optimal distribution of  $\tau_{\kappa}$  is obtained, the mass of each different type of aerosol has to be adjusted in each grid cell. Since we do not have additional information as to which type of aerosol causes the mismatch between the observed optical depth and the model optical depth we choose to adjust each aerosol type i proportional to its mass M in gridcell k:

$$\boldsymbol{M}_{ik}^{a} = \boldsymbol{M}_{ik}^{fc} \frac{\boldsymbol{\tau}_{k}^{a}}{\boldsymbol{\tau}_{k}^{fc}} . \tag{2.5}$$

This assumption, which was also made by Collins et al. (2001), may be relaxed in future versions when multiple wavelength optical depth observations are assimilated (see chapter 5). Optical depths at different wavelengths carry information on the aerosol type because the extinction has a spectral dependence that depends on the aerosol types that are present in the atmospheric column.

# 3 Results of phase 1

#### 3.1 Introduction

The Indian Ocean Experiment (INDOEX) was selected to test the prototype assimilation system. INDOEX (Ramanathan et al, 2002) was undertaken in February and March 1999 with the objective to determine the pollution outflow from India over the Indian Ocean, and to assess its radiative impact. The chemical and optical properties of the aerosols were studied by performing a large number of in-situ observations both on the ground and during aircraft flights. In addition satellite and ground-based remote sensing instruments made nearly continuous measurements. The vast amount of data that was collected during the intensive field phase contains valuable information that can be used to evaluate all parts of the assimilation system: the retrieval, the chemistry/transport model and the assimilation procedure.

In phase 1 of ARIA only a first brief evaluation of the assimilation system is made using INDOEX data. A more extensive evaluation of the system will be made in phase 2 of the project.

The results of the three modules, i.e. retrieval, modelling, and assimilation are presented and discussed below in sections 3.2, 3.3 and 3.4.

# 3.2 Retrieval of aerosol properties

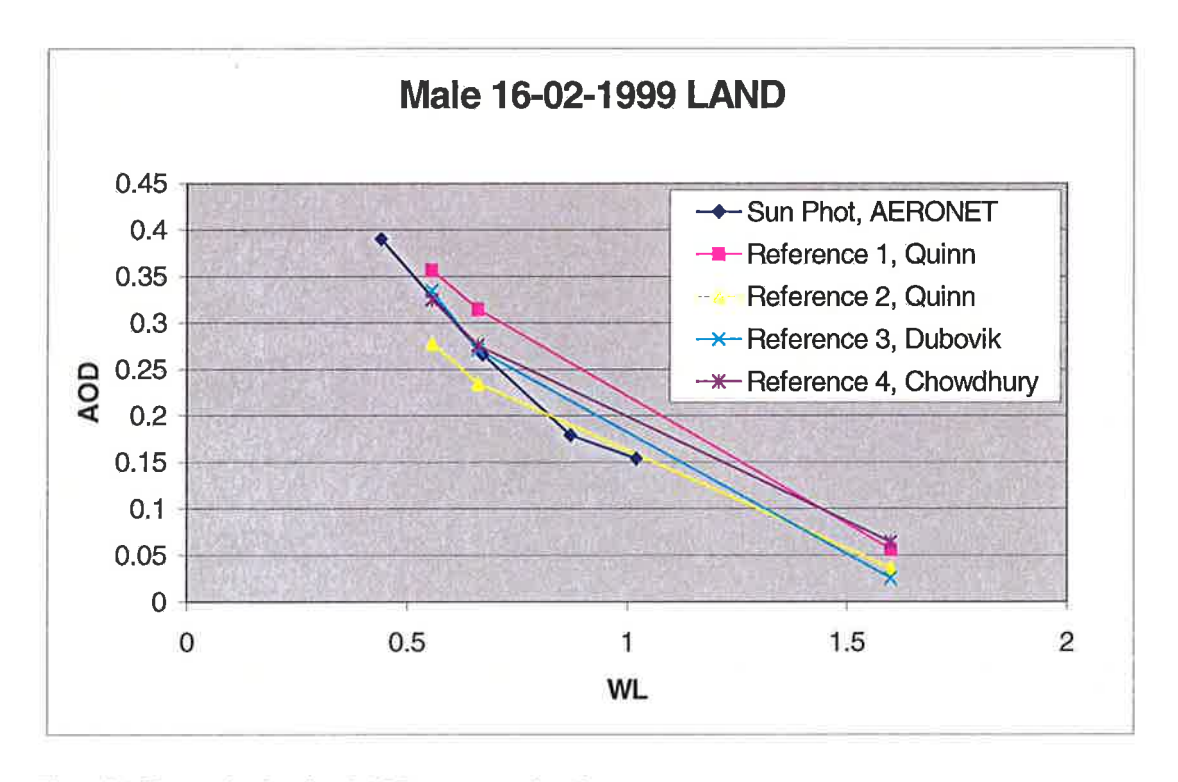


Figure 3.1 Observed and retrieved AOD versus wavelength

In Figure 3.1 preliminary results from the dual view algorithm are compared with AERONET (Holben et al., 1998) ground based sun-photometer data for February 16 at Male Island (4.19° N 73.53° E). The time

difference between the sun photometer measurements and the satellite overpass was 55 minutes. A homogeneous AOD area over Male Island at around 8km distance from the sun photometer was selected to retrieve the AOD. Preliminary results based on Quinn et al., 2001, using the North Hemispheric Indian Ocean (NHIO) aerosol type show that the table computed based on optical measurements (figure 3.1, reference 1) overestimates the AOD while the one based on chemical measurements (figure 3.1, reference 2) underestimates the AOD at the shorter wavelength. In both cases AOD values agree within 0.05 at 0.659  $\mu$ m. For the computation of the AOD based on Dubovik et al., 2002, data (figure 3.1, reference 3) two aerosol types were used: sea salt (SS) aerosol and the Maldives aerosol mixture (MM) at the KCO. Comparison of the results with AERONET derived AOD at 0.659  $\mu$ m shows very good agreement (within 0.01). The AOD retrieved based on Chowdhury et al., 2001, (figure 3.1, reference 4) agrees also within 0.01 at 0.659  $\mu$ m with AERONET results for a wavelength of 0.659  $\mu$ m. From figure 3.1 we could conclude that the Maldives mixture and the sea salt aerosols (figure 3.1, reference 3) are the most appropriate for this area. Unfortunately no other collocated sun photometer data are available to compare with the retrieved AOD in February 1999.

Both the single and dual view algorithms have been applied to process the data over the ocean, whereas over land only the dual view algorithm was applied. The initial choice for the dual view algorithm over the ocean was made because the comparison with the sun photometer data suggested that this would give the best results. Only one such comparison is available which is insufficient for a sound judgement on the best applicable algorithm. Furthermore, as indicated in Robles Gonzalez et al. (2000), the dual view algorithm yields values that are too high over turbid coastal waters (case II waters, see also Pasterkamp et al., 2000). Hence near the land-water transition there was a discontinuity in the AOD with higher values over significant parts of the ocean. In addition, because of the small swath of the nadir view over the ocean (approximately one third of the normal swath), not enough data were available for complete coverage during the month. Therefore also the single view algorithm was applied over the ocean and the results were combined with those over land from the dual view algorithm.

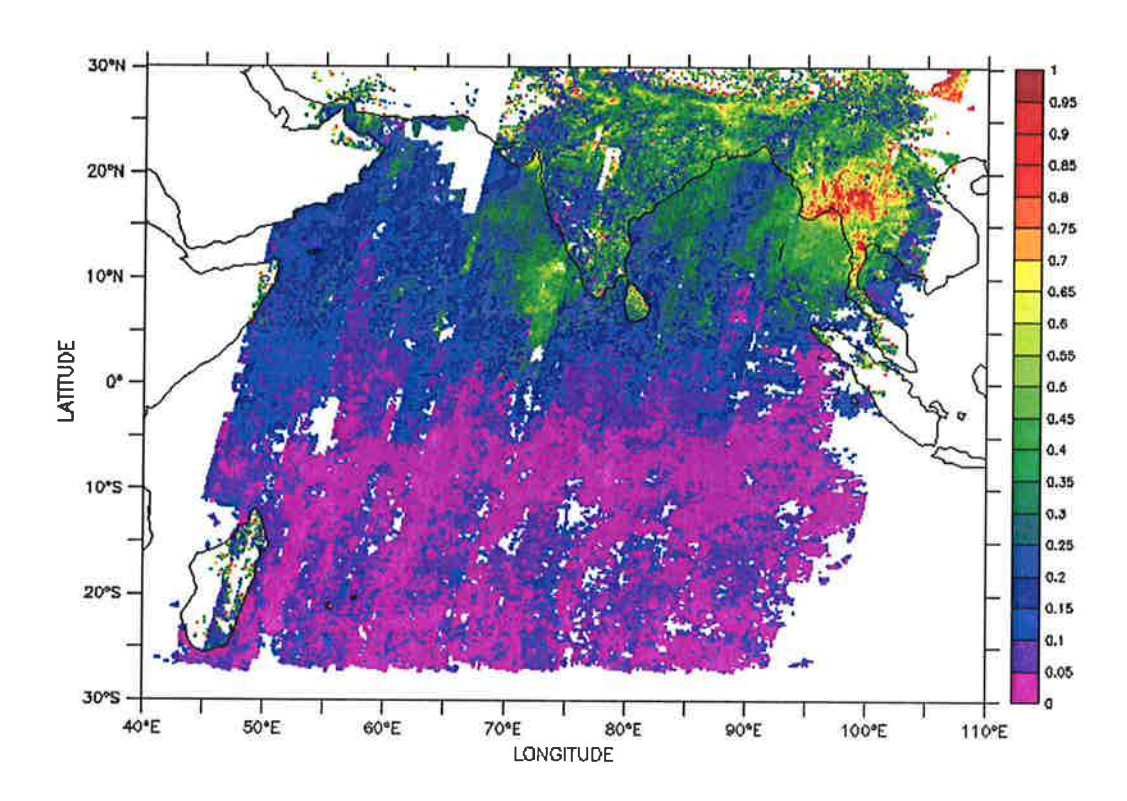


Figure 3.2: Results of AOD retrieval at 659 nm, averaged over February 1999.

The results at the wavelength of 659 nm are shown in figure 3.2. This wavelength was chosen here in order to compare with the 3-month average based on AVHRR retrieval that was presented in Rajeev and Ramanathan (2001). The mean AOD over the INDOEX area for February was obtained as the average of all available ATSR-2 data. With one overpass every three days, and further reduction of the available data due to contamination by clouds or sunglint, these averages represent all valid data points, are snapshots at the time of the ATSR-2 overpass (around 6:00 a.m. UTC). The original AOD values, with a resolution of 1x1 km², were averaged to a 10x10 km² grid. The retrieval method used was described in Robles Gonzalez et al. (2000). The AOD over land was retrieved using the new dual view algorithm. Over water the new single view algorithm was applied. The white areas in Figure 3.2 contain no data due to the presence of clouds, sunglint or because no data was processed over the area (upper left and lower right corners).

Over land, the AOD values at 659 nm in figure 3.2 range between about 0.2 and 0.4 over most of the region. For continental air masses the contribution of black carbon and water soluble aerosols, mainly from anthropogenic origin, is high. AOD values up to 1 are observed over Myanmar and Thailand due to the occurrence of intense fires producing biomass burning aerosol in this season.

Over the ocean AOD values up to 0.6 are observed close to land. These high values are most likely due to aerosol advected from the Indian peninsula. During the winter monsoon northeasterly winds prevail over the Indian Ocean. These winds export polluted and anthropogenically influenced air masses in 5 to 10 days from Arabia and the Indian subcontinent to large areas of the Indian Ocean and the Arabian Sea. The AOD near the coast is similar to that over land, and gradually decreases away from the land due to the absence of aerosol sources.

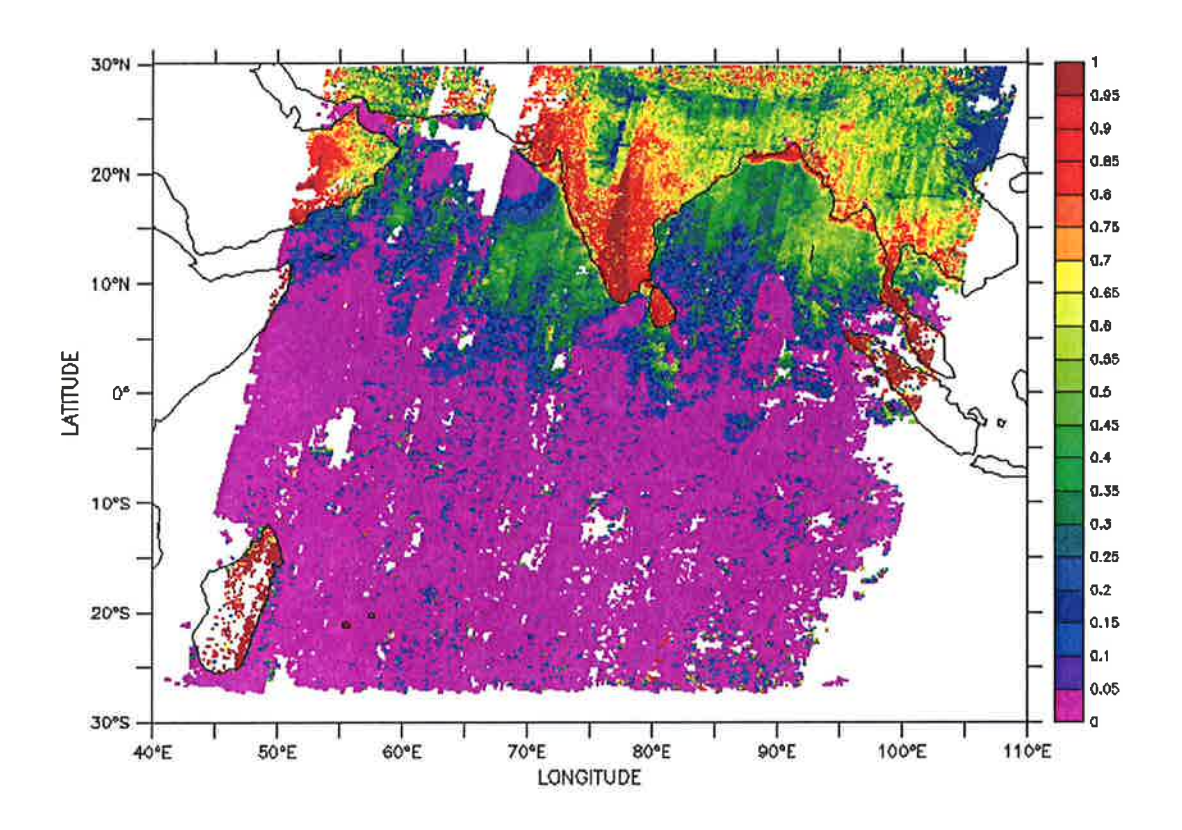


Figure 3.3: Retrieved relative contribution of continental aerosol (KCO) to the total TOA reflectance.

Figure 3.3 shows the relative contribution of the KCO aerosol type to the TOA reflectance measured by the satellite. The algorithm selects this relative contribution using the least squares method. A value of 1 means that the only aerosol selected is the KCO aerosol type, zero means that the aerosol that best fits the measured reflectance is the sea salt. In figure 3.3 we can see values along the coasts of about 0.8-1 near the west coast of India, south of Bangladesh and Myanmar due to aerosols advected from the land. Continental contribution decreases gradually with the distance to the continent showing the large influence that anthropogenic aerosols have over pristine areas. Figure 3.3 shows a strong gradient of the aerosol composition from north to south. This gradient illustrates the high continental influence over the Indian Ocean and Arabian Sea.

Over the southern hemisphere relatively high AOD values can also be observed in figure 3.2, even as far south as 5°S, in good agreement with Rajeev and Ramanathan, 2001, who used AVHRR data to retrieve the AOD for the INDOEX period. Low and relatively quite constant AOD values can be observed in figure 3.2 south of 5°S. For comparison, 3 values for the the average AOD are available. Quinn et al., 2001, on board the RV Ronald H. Brown measured the AOD using a 5-channel hand-held Microtops sun photometer Mean **AOD** values Co.). reported (available through http://www.joss.ucar.edu/codiac) over the area from 23° S to 10° S and from 54° E to 59° E were 0.07± 0.01 at 675 nm. Mean AOD retrieved from ATSR-2 data with the single view algorithm over the same area was  $0.06 \pm 0.02$  at 659 nm. The good agreement with Quinn et al. (2001) measurements and the relatively homogeneous AOD spatial distribution which is in good agreement with results presented by Rajeev and Ramanathan (2001) give confidence in the results shown in this report.

# 3.2 Aerosol modelling

#### 3.2.1 Emission inventory – sources

The chemical transport model (TM3) has been extended in phase 1 of ARIA with carbonaceous aerosol. In recent studies and experiments it was found that the organic carbon mass concentration may be of the similar magnitude as that of sulfate in both anthropogenically influenced areas and remote areas (Novakov and Corrigan, 1996, Hegg et al. 1997). Four types of carbonaceous aerosol were added to the TM3 model. We differentiate between black carbon (BC), a soot-like aerosol containing mainly elemental carbon, and organic carbon (OC). Both BC and OC can be hydrophobic (insoluble in water) and hydrophilic (water soluble).

The ratio between black and organic carbon may not be constant in the atmosphere because of different lifetimes and sources. Penner et al. (1995) have shown that radiative forcing is quite sensitive to the ratio of BC to OC emissions.

The sources of BC and OC sub-micron aerosol particles were taken from the work of Cooke et. al. (1999). They provide global-scale emissions of carbonaceous aerosol from fossil fuel usage with a resolution of 1° x 1°. The quantity of carbonaceous aerosol emitted by fossil fuel combustion is proportional to the quantity of fuel consumed and the emission factor for the combustion process. The quantity of fuel consumed is reasonably well known (e.g. United Nations, 1993). The distinction between BC and OC emission factors for the Cooke (1999) emission data, is based on fuel type (e.g. diesel, kerosene, coal, gas), consuming sector (domestic, transport, and industry), and level of development of the country.

The inventory of Cooke et al. (1999) does not include natural sources of carbonaceous aerosol nor secondary production of carbonaceous aerosol from gaseous emissions from natural and anthropogenic sources. However, secondary production of OC aerosol probably contributes a large fraction of the OC aerosol mass. This is confirmed in a comparison between modeled and measured concentrations of OC and BC (Cooke et al., 1999). It is shown that modeled concentrations of OC for both marine and rural sites are greatly underestimated. The ratio between the modeled and measured OC concentrations for the rural and marine sites is of the order of 0.17 in both cases. However, for the same areas the average measured to modeled ratio for BC is close to unity. This indicates that the Cooke et al. emission inventory for anthropogenic carbonaceous aerosol gives reasonable values, whereas secondary production or the natural sources of OC results in a large discrepancy for this aerosol type. The comparison between measured and modeled OC concentrations indicated that these additional sources increase the concentrations of particulate OC by a factor of 4-5 in remote and rural regions. The ratio of modeled to measured OC in urban areas is approximately

0.33, corresponding to an increase in the OC concentration due to secondary and natural sources by a factor of 3. As a first approach we have chosen to increase the burden of organic carbon aerosol by multiplying the emissions by a factor of 4.

Apart from the distinction between OC and BC we distinguish hydrophobic and hydrophilic aerosol. Hydrophobic aerosol will neither be activated as cloud condensation nuclei, nor will it be scavenged by precipitation. Particulate carbon is predominantly hydrophobic, but a certain fraction of the emissions may be hydrophilic (Cachier, 1998). Accordingly we assume that 80% of the emitted BC is hydrophobic and 20% is hydrophobic. OC is emitted in equal proportions of hydrophobic and hydrophilic aerosol (Cooke et al., 1999). The emissions are evenly spread over the year. Figures 3.4a through 3.4d show the emissions of carbonaceous aerosol species for the model resolution and time-step used in this work.

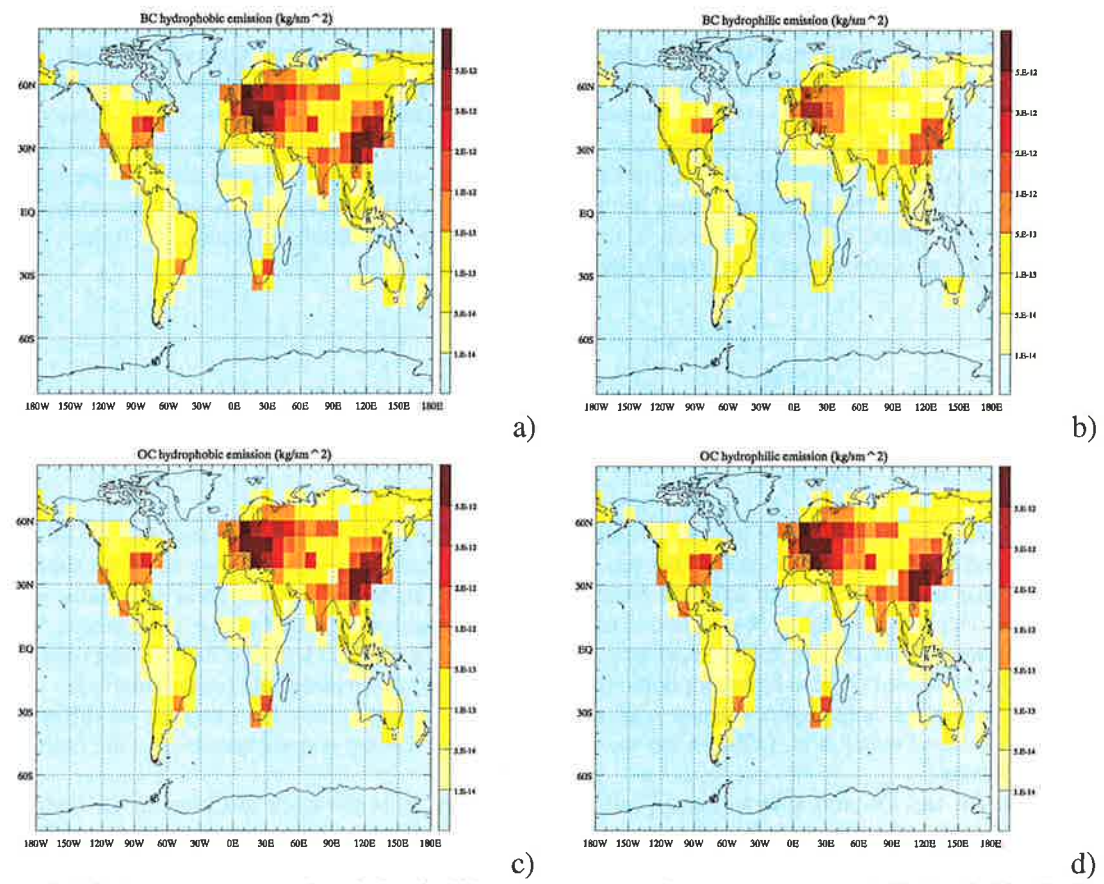


Figure 3.4 Carbonaceous aerosol emission in kilograms per second per square meter: a) Hydrophobic black carbon, b) hydrophilic black carbon, c) hydrophobic organic carbon, and d) hydrophilic organic carbon.

# 3.2.1 Dry and wet deposition – sinks

The aging process for both BC and OC is represented by a first order transformation of hydrophobic to hydrophilic aerosol with an exponential lifetime of 1.15 days. Moreover, the aerosol lifetime is assumed to be governed by wet and dry deposition, which means that we do not consider additional chemical sinks.

#### Dry deposition

Both hydrophilic and hydrophobic aerosol are removed from the model atmosphere by dry deposition. Dry deposition is interpreted in terms of an electrical resistance analogy, in which the transport of material to the surface is assumed to be governed by three resistances in series: the aerodynamic resistance, the quasi-laminar layer resistance, and the surface or canopy resistance. The total resistance of a (gaseous) species is the sum of the three individual resistances and is, by definition, the inverse of the deposition velocity. The

actual dry deposition flux, the amount of material deposited to a unit surface area per unit time, is directly proportional to the product of this velocity and the concentration of the deposited species at some reference height above the surface. The dry deposition scheme in TM3 is described by Ganzeveld and Lelieveld (1995) and Ganzeveld et al. (1998). The scheme was originally developed for ECHAM and has been validated with sulfate observations by Jeuken (2000). Results of the dry and wet deposition scheme in TM3 for black and organic carbon, accumulated over February 1999 are shown in figure 3.5.

#### Wet deposition - Below cloud

Below-cloud scavenging of aerosols by falling precipitation, usually referred to as rainout, depends on raindrop size and aerosol particle size and a corresponding collection efficiency. The collection efficiency, E, for sub-micron aerosols in the accumulation mode is usually small. These aerosol particles are too large to have an appreciable Brownian diffusivity and also too small to be collected effectively by either impaction or interception.

Dana and Hanes (1976) give the theoretical mass rainout coefficients integrated over the rain droplet and aerosol size spectra. We assumed a frontal rain spectrum with geometric mean radius r=0.02 cm and  $\sigma$  = 1.86 and a lognormal aerosol distribution with r = 0.14  $\mu$ m and  $\sigma$  = 2 (Jeuken, 2000 and references therein). With these numbers the mass rainout coefficient normalized to unit rainfall rate then becomes 0.05 mm<sup>-1</sup> (Dana and Hanes, 1976).

The scavenging coefficient (s<sup>-1</sup>) is the product of the normalized mass rainout coefficient and the local rain flux. The below-cloud scavenging rate, the amount of material lost from a column of air with unit surface area per unit time, is directly proportional to the vertically integrated product of the scavenging coefficient and the concentration.

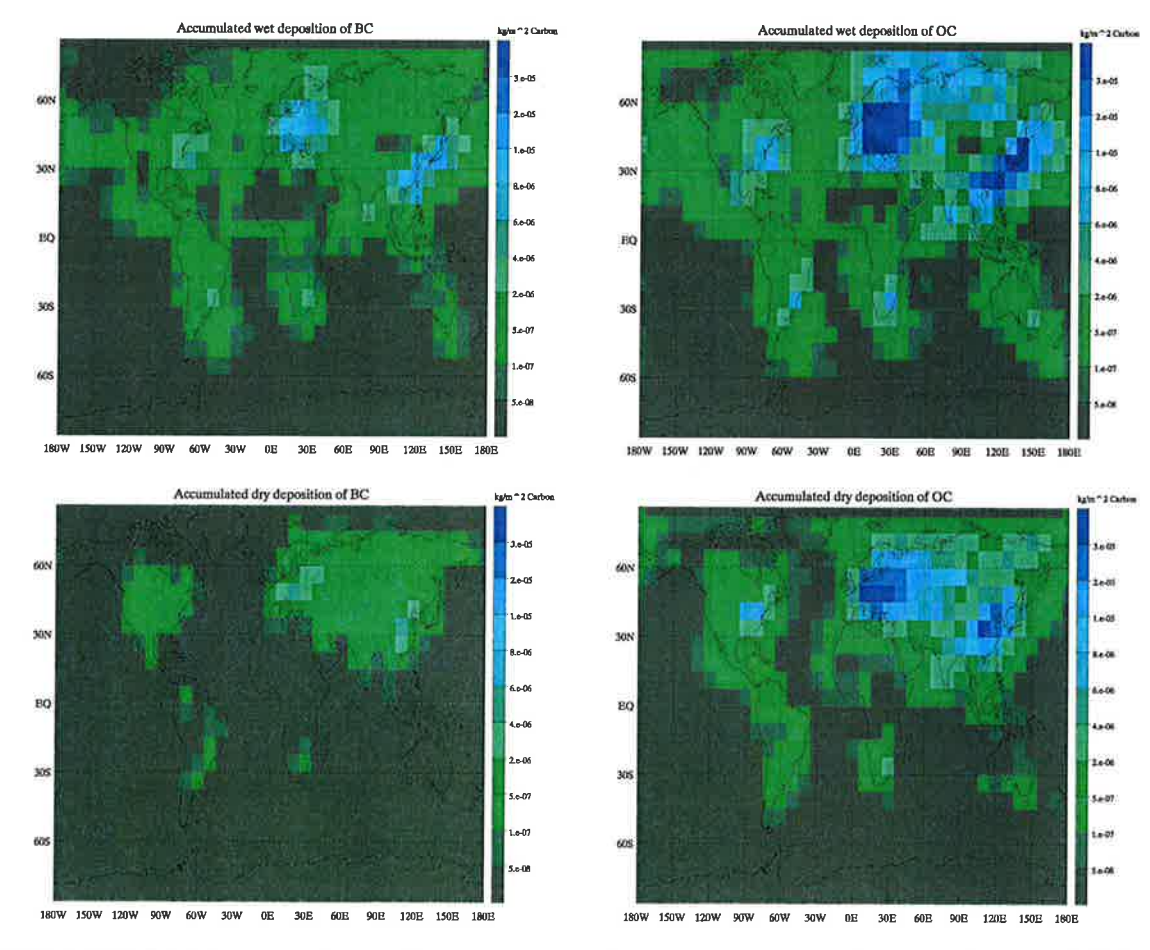


Figure 3.5 Modeled dry and wet deposition of organic and black carbon, accumulated over February 1999, without assimilation of AOD observations.

#### Wet deposition - In cloud

To calculate washout (also called in-cloud scavenging) a distinction is made between precipitation formation in convective clouds and in and large-scale clouds. For convective clouds, in-cloud scavenging is evaluated using the mass fluxes calculated in the convective cloud scheme. It is assumed that aerosol, transported in the updrafts, dissolves in the liquid (cloud and rain) water present. Scavenging efficiency values,  $\eta$ , of Balkanski et al. (1993) and Guelle et al. (1997) are adopted, i.e.  $\eta_{deep} = 70\%$  for deep convection and  $\eta_{shallow} = 0.5*$   $\eta_{deep}$  for shallow convection (Jeuken, 2000).

The large-scale in-cloud scavenging through precipitation is based on the work of Roelofs and Lelieveld (1995). In-cloud scavenging of aerosols is the result of a number of sequential processes. Firstly, cloud condensation nuclei (CNN) grow to cloud droplets, the so-called nucleation scavenging. Secondly a fraction of the remaining aerosols is collected by the cloud droplet due to interstitial scavenging. The third step is the actual removal; the rate conversion of cloud water to precipitation.

Particles larger than 0.5 micron, representing most of the aerosol mass, become cloud droplets in a typical cloud (Seinfeld and Pandis, 1998). Indeed, nucleation scavenging is very efficient for particles larger than 50 nm. On the other hand, interstitial aerosol collection by cloud droplets is rather slow and often scavenges a negligible fraction of the interstitial aerosol mass. However, aerosol particles smaller than 50 nm have short lifetimes in clouds due to Brownian diffusion. Very fine particles, numerous in source regions, will therefore be captured in the cloud droplets during the cloud lifetime. The combined process of nucleation and interstitial aerosol scavenging is very efficient, often incorporating most of the aerosol number and mass in cloud droplets. In order to calculate the in-cloud aerosol scavenging coefficient, we use the in-cloud scavenging scheme of Roelofs and Lelieveld (1995), where we treat (hydrophilic) aerosol as a completely soluble species.

The transformation of cloud water to precipitation due to coalescence of cloud drops is simply the ratio between the precipitation formation rate and the cloud water content.

The final in-cloud scavenging rate is determined by the slowest of the two processes: aerosol to cloud-drop conversion or cloud-drop to precipitation. For aerosols the transformation of cloud to rain water is the rate determining step.

Results of the below-cloud and in-cloud scavenging are presented in figure 3.5.

### 3.4 Aerosol assimilation

The retrieval of the optical depths from the ATSR-2 data and the TM3 model that were used in the test runs are described in chapter 2.2 and 2.3 respectively. obtaining results of the prototype assimilation system requires the integration of three parts: the retrieval, the chemistry-transport model and the assimilation procedure. The model was run for one month, -February 1999. Since the lifetime of the aerosols is relatively short, there was no need for a long spin-up period. Two runs were made: a free run without assimilation of observations, and a run that included the assimilation of the ATSR-2 optical depths at 656nm. Observational data was available from a window of 30°N-30°S and 40°E-100°E. On most days there were two satellite overpasses in this domain roughly 2 hours apart. The observational data was assimilated at 6:00 UTC each day.

Figures 3.6 to 3.9 show the global distribution of aerosol optical depths at 656nm, on 4 consecutive days. Upper left panels are the results from the free run, without assimilion of observations. The industrialised areas in western Europe, Asia and the US have the highest values, although the US values seem too low (most of the time less than 0.1). Values in Europe and Asia do not exceed 0.4. The limited aerosol lifetime is reflected by the fact that relative high values are located near industrial regions.

The upper-right and lower-right panels show results from the run including assimilation just before and just after a new set of observations are assimilated. The 24-hour AOD forecast (upper-right) is used during the assimilation of the ATSR-2 observations (shown in the lower-left panels), yielding the analysed distribution of AOD. It is clear that there is a fairly large model bias in the INDOEX domain. Nearly all observed AOD values are larger than the forecasted values. The assimilation procedure is a strong source of aerosol in the model. Although the effect is strongest in the INDOEX domain, advection of the aerosol also affects the

AOD in the eastern Pacific Ocean. Note however that the model does not contain any source of aerosol over water (no sea salt), so that any change of aerosol mass due to advection will have a large relative impact, although the absolute value of the AOD over these remote areas is still small.

Since in the assimilation procedure we use a correlation length scale of 500km (which is short compared to the coarse resolution of the horizontal grid) the impact of the observations is restricted to gridcels covered by the satellite overpasses. The 24 hour forecast carries still quite some information from the assimilated observations during previous days, since the forecast is much closer to the new observations than the free run. This means that the aerosol lifetime in the model is probably sufficiently long to fill the gap of 3 days between two satellite observations at the same location.

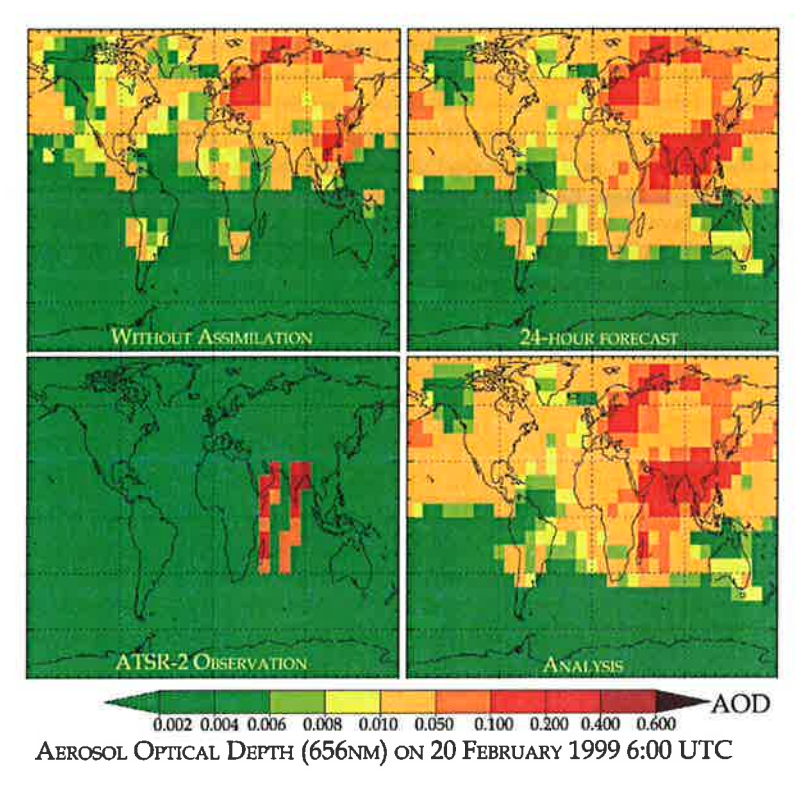


Figure 3.6 Aerosol optical on February 20, 1999, 6:00 UTC, as calculated by a free run of the model (without assimilation), a 24-hours forecast, the ATSR-2 observation aggregated to the TM-grid, and the analysis.

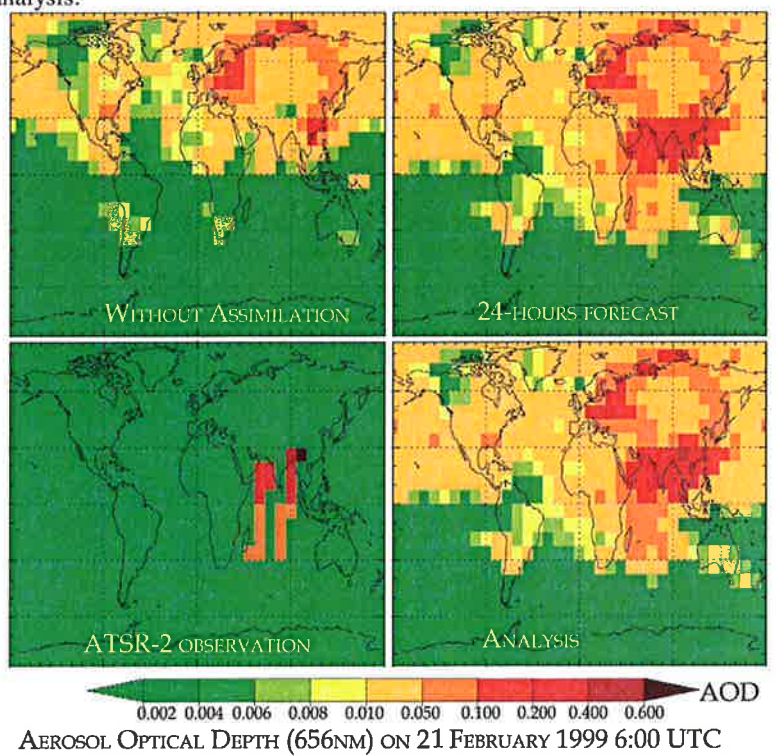
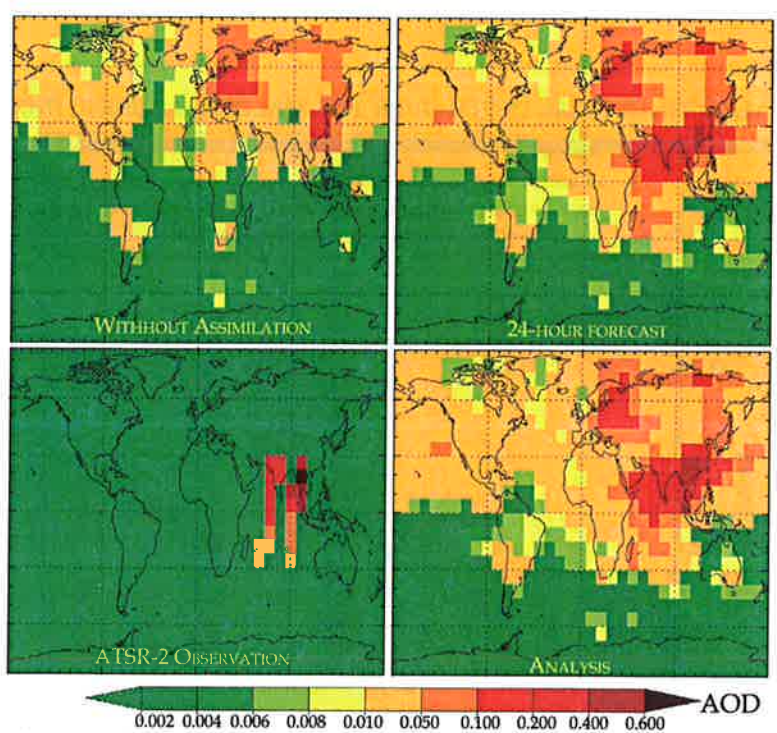


Figure 3.7 Same as figure 3.6, but for February 21, 1999, 06:00 UTC



0.002 0.004 0.006 0.008 0.010 0.050 0.100 0.200 0.400 0.600 AEROSOL OPTICAL DEPTH (656NM) ON 22 FEBRUARY 1999 6:00 UTC

Figure 3.8 Same as figure 3.6, but for February 22, 1999, 06:00 UTC

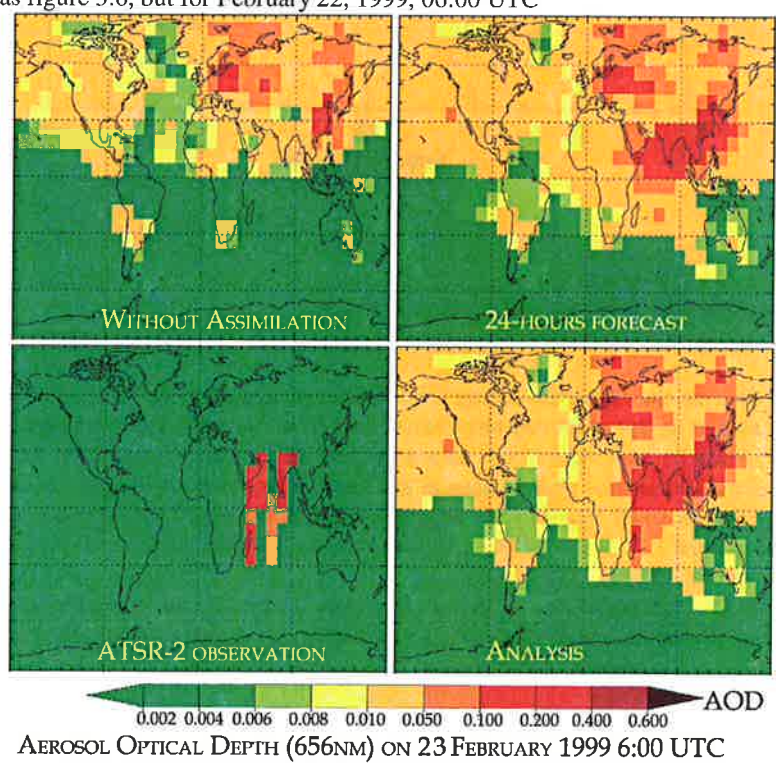


Figure 3.9 Same as figure 3.6, but for February 23, 1999, 06:00 UTC

#### AEROSOL OPTICAL DEPTH OVER THE MALDIVES DURING INDOEX

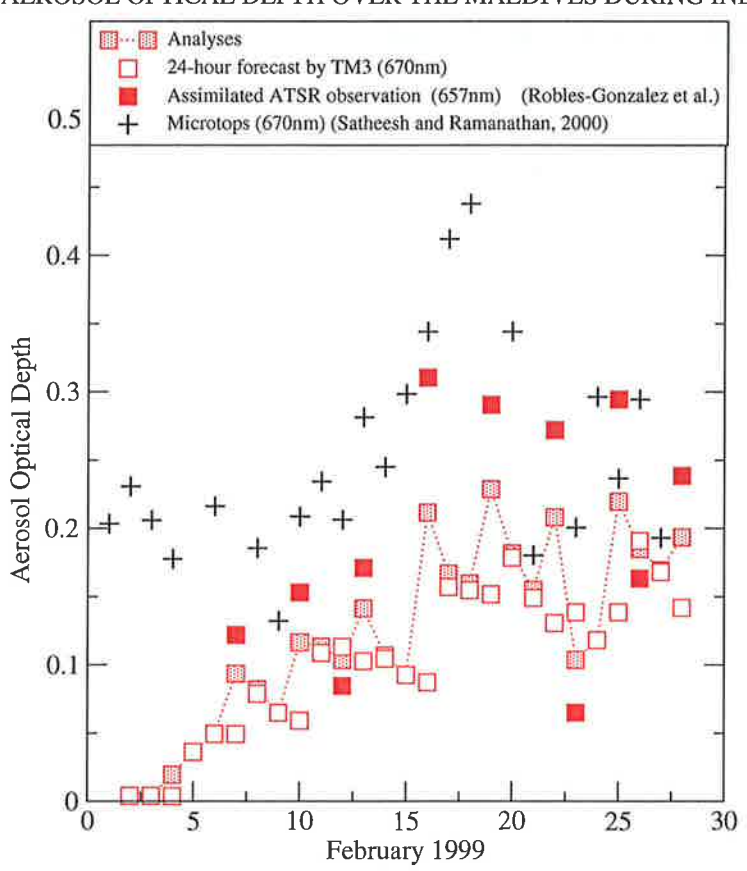


Figure 3.10 Aerosol optical depth at 656nm in February 1999.

In figure 3.10 the AOD over the Maldives during INDOEX is plotted, i.e. the forecasts, the analyses, the assimilated observations and independent sun photometer data from Satheesh and Ramanathan (2000). This plot illustrates the fact that the assimilation acts as a source of aerosol in the model on most days. Model values nearly always decrease when no observations in this specific grid cell are assimilated (e.g. February 8-10,14-16, and 17-19). Only a small impact is found when there is a ('super') observation available for an adjacent gridcell (e.g. February 8, 14, 17, 18), reflecting the small model forecast error correlation length scale used in the assimilation.

The observations made by the Microtops sun photometer from Satheesh and Ramanathan produce higher values in the first half of February, compared to the assimilated ATSR-2 observations. Note however that the Microtops data are 6-hourly averaged point values and not area averages like the aggregated ATSR observations. During the first days of the simulation the model AOD values are much lower than observed by the sunphotometer. During these days this specific grid cell was not yet affected by the observations This gives an indication of the large bias between the model and the observations which was also found from figures (3.6 to 3.9).

# 4 Conclusions of phase 1

The objective of the first phase was to deliver a working assimilation system for aerosol optical depth observations. The complete system consists of three main modules: (1) the AOD retrieval algorithm, (2) the aerosol chemistry-transport model, and (3) the assimilation module. Even though the duration of phase 1 of ARIA was short, only 8 months contrary to the original planning for one year, significant progress has been made for all three modules. The working prototype of the system integrating the three modules is demonstrated by the application to INDOEX. Next sections summarize the results and conclusions of the three workpackages.

#### 4.1 Aerosol retrieval

- LUT's for the aerosol reflectance at several wavelengths and sun-satellite geometry's have been developed to retrieve AOD values from ATSR-2 radiometer data over the Indian Ocean.
- The cloud detection algorithm from Koelemeijer and Stammes (1999) has been automated.
- A single component method for retrieval is not possible due to coupling effects.
- Chemical and optical measurements were combined to create a set of LUTs that best define the aerosol
  properties in the region. KCO aerosol mixture and sea salt particles were used in the new algorithms to
  retrieve the AOD over the INDOEX area for February 1999.
- AOD values retrieved over Male in the Maldives Republic on February 16 1999, were compared with AERONET ground-based measurements. Results agree within 0.05 at 0.659 μm.
- Mean AOD values over the INDOEX area for February 1999 retrieved using the new dual view algorithm over land and the new single view algorithm over water have been shown. High AOD values of about 0.4 are observed over most of the continent. Over Myanmar and Thailand AOD observed values of up to 1 are due to biomass burning aerosols. High AOD values are also observed over the Indian Ocean and the Arabian Sea up to 5°S due to export from the continent. At lower latitudes, far away from the continent, AODs of about 0.1 are observed. Hence the results show that anthropogenic emissions in SE Asia influence a vast part of the Indian Ocean.
- Gradients of the aerosol loading and chemical composition are observed over the INDOEX region, with aerosol concentrations decreasing from northern to southern latitudes. KCO aerosol type prevail over the northern INDOEX area down to 5°S while sea salt aerosol predominate in southern latitudes.
- These results are in good agreement with the results obtained during the INDOEX campaign itself.

# 4.2 Aerosol modelling

- The chemical transport model TM3 is reconstructed in such a way that new aerosol types can be easily
  included.
- TM3 has been extended with four carbonaceous aerosol types: organic and black carbon in hydrophobic and hydrophilic form
- Based on comparison between modelled and measured carbonaceous aerosol concentrations the secondary production and natural sources of carbonaceous aerosol have been included by multiplying the carbonaceous aerosol sources with a factor of 4.
- Aging of aerosols is taken into account by transfer of hydrophobic to hydrophilic carbonaceous aerosol with an exponential lifetime of 1.15 days.

#### 4.3 Assimilation of AOD

- The Optimal Interpolation assimilation method that has been implemented in combination with the aggregated ('super'-) observations yield a fast, computationally efficient method for the integration of optical depth model results and observations.
- The assimilation of satellite observed AOD clearly improves the 24-hour forecasts of the optical depths in the INDOEX domain.
- The lifetimes of the aerosol types present in the model are long enough to carry the observational information for several days. The model is thus able to fill in the gaps between satellite overpasses. This is an important result since it demonstrates the feasibility of our approach.
- The free model run yields much smaller optical depths than the values that are retrieved from the ATSR-2 instrument. This bias between model and observations needs to be reduced. There are several explanations for the strong bias between the model free run and the observations. Part of phase 1 of the project was the introduction of 4 types of carbonaceous aerosol in the model, some types of aerosols are still missing: dust and sea salt, which are foreseen to be implemented in phase 2. Moreover, natural emissions and emissions from biomass burning are not yet properly taken into account. ATSR observations show many fires in China and Central Asia and central Africa during the INDOEX episode, that likely affect the observed optical depths significantly. Another explanation for the bias might be related to the assumptions made for optical properties of the aerosols, since these are highly uncertain.

# 5 Outlook to phase 2

The main goal of phase 1 of the ARIA project was the preparation of a working prototype system for the retrieval and assimilation of aerosol data. This prototype has been finished and results were presented in previous chapters. Obviously the prototype requires improvement and extensive evaluation before it can serve as the tool that was intended: a system for the production of satellite retrieved aerosol data and of the global distribution of the main aerosol types.

For each of the three main parts of the system, the retrieval module, the chemistry/transport model and the assimilation module, improvements are foreseen in the next phase of the ARIA project.

#### Retrieval

The information provided by the model about the distribution of aerosols (aerosol profiles and aerosol types) will be used for specification of the initial assumptions required by the aerosol retrieval algorithm. The model information will also be used to select those pixels for retrieval, where retrieval errors can be expected to be small, e.g. because one specific aerosol type is strongly dominant. The combined use of transport modelling and aerosol retrieval can yield aerosol products that are superior to current products that use climatological or hypothetical information in the retrieval.

#### Model

The source distributions of all relevant aerosols will be refined (e.g. by introducing a seasonal cycle) and evaluated. Higher resolution model forecast may also improve the performance of the assimilation system, and can easily be implemented. Dust aerosol and sea salt aerosol will be introduced in the model. Better estimations of the natural emission and secondary formation of carbonaceous aerosol are also planned.

#### Assimilation

A detailed evaluation of the assimilation system is planned, focussing on the appropriate parameter settings, prescribed constant or advected error distributions etcetera. Here the recent measurement campaigns like

INDOEX, ACE-1, ACE-2 and ACE-Asia, can provide valuable independent observational data both on the optical depths as well as the aerosol mass distributions.

Finally, the assimilation of multiple wavelength optical depths may in principle provide useful additional information on the mixtures of aerosol types present the atmosphere. Further research in phase 2 of ARIA is needed to determine whether the uncertainties in optical properties of the different aerosol types is small enough to extract this information. This will first be tested in a one-dimensional environment (profiles). When it has been shown that the assimilation results improve using multiple wavelength observations from SCIAMACHY, the multiple wavelength option will be included in the three-dimensional assimilation system.

A schematic representation of the assimilation system as proposed in this paragraph is depicted in figure 4.1. In the proposed system the model forecast of the 3-dimensional aerosol distribution will be used as a priori information for the retrieval algorithm (thick grey arrow). The 2 new products, the retrieved and the assimilated aerosol distribution, will be derived in this second phase, and will be evaluated against independent observations such as from the AERONET network and measurement campaigns like INDOEX, ACE and TARFOX. The feedback of assimilation on retrieval is a new and very promising prospect of the next phase system.

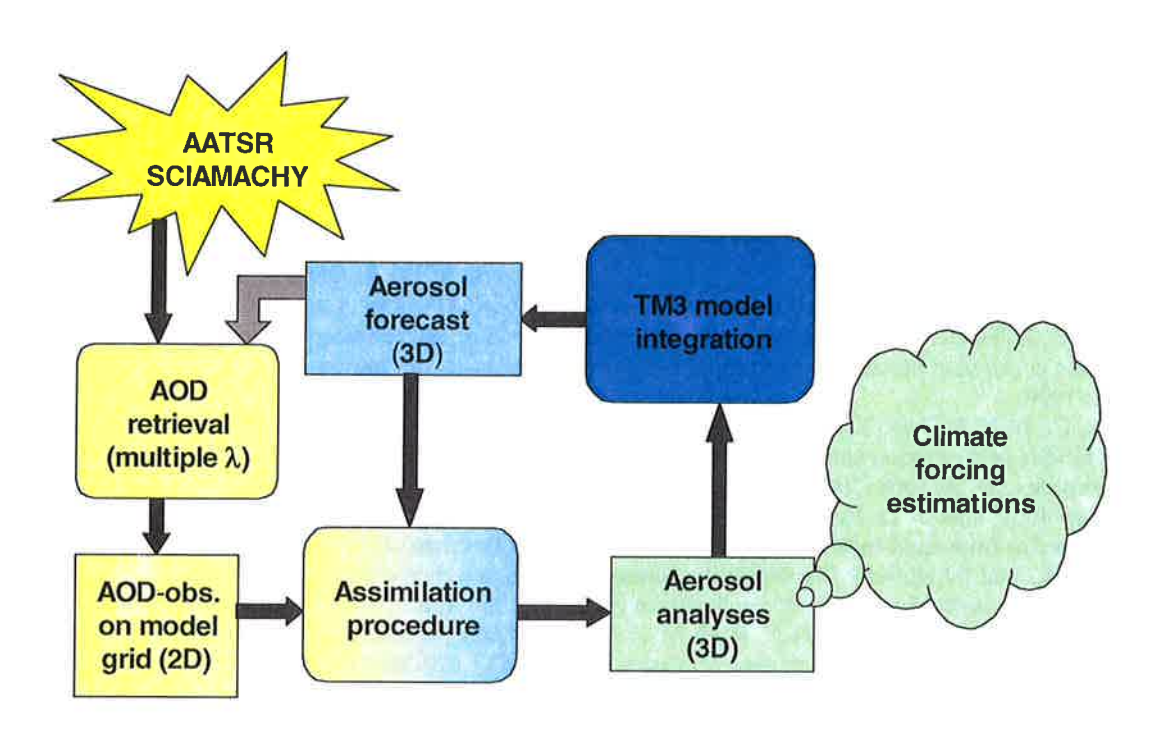


Figure 4.1 The Aerosol retrieval and assimilation system as proposed for implementation in phase 2 of ARIA.

#### Acknowledgements

We are grateful to Henk Eskes for helping us adapt his optimal interpolation scheme for assimilation of ozone for aerosols. We also gratefully acknowledge the guidance provided by the ARIA Advisory Group, consisting of Prof. Dr. P. Builtjes, Dr. H. ten Brink, Dr. H.van der Woerd and Dr. H. Slaper.

#### References

- d'Almeida, G.A., P. Koepke, and E.P. Shettle: Atmospheric aerosols: Their global climatology and radiative characteristics. A. Deepak. Hampton, Va. (1991).
- Balkanski, Y.J., D.J. Jacob, G.M. Gardner, W.C. Graustein, and K.K. Turekian: Transport and residence times of tropospheric aerosols inferred from a global three dimensional simulation of <sup>210</sup>Pb. J. Geophys, Res. 98, 20573-20568 (1993).
- Brink, H.M. ten, A. Hensen, A. Khlystov, R. van Dorland, A. Jeuken, P. van Velthoven, J. Lelieveld, A. van den Berg, D.P.J. Swart, J.B. Bergwerff, and A. Apituley: Aerosol: Cycle and Influence on the Radiation Balance. NOP-final report (2001).
- Cachier, H.: Carbonaceous combustion particles. In: Atmospheric Particles, 295-348. Eds. R.M. Harrison, and R.E. Van Grieken, John Wiley, New York (1998).
- Chowdhury Z., L. S. Hughes, and L. G. Salmon: Atmospheric particle size and composition measurements to support light extinction calculations over the Indian Ocean. J.Geophys.Res. 106, 28597-28605 (2001).
- Collins, W.D., P.J. Rasch, B.E. Eaton, B.V. Khattatov, J-F. Lamarque and C.S. Zender: Simulating aerosols using a chemical transport model with assimilation of satellite aerosol retrievals: Methodology for INDOEX. J. Geophys. Res. 106, 7313-7336 (2001).
- Cooke, W.F., C. Liousse, H. Cachier, and J. Feichter:: Construction of a 1x1 degree fossil fuel emission data set for carbonaceous aerosol and implementation and radiative impact in the ECHAM4-model. J. Geophys.Res. 104, 22,137-22,162 (1999).
- Dana, M.T., and J.M. Hales: Statistical aspects of the washout of polydisperse aersosols. Atm. Env. 10, 45-50 (1976).
- De Leeuw, G., C. Robles Gonzalez, J. Kusmierczyk-Michulec and R. Decae (2002a). Satellite Retrieval of Aerosol Properties, EGS, Nice, April 2002.
- De Leeuw, G., C. Robles Gonzalez, J. Kusmierczyk-Michulec and R. Decae (2002b). Retrieval of aerosol properties and their use in chemistry transport models, Workshop on Chemical Weather Forecasting, DLR, Oberpfaffenhofen, Germany, 7-8 May, 2002.
- De Leeuw, G., C. Robles Gonzalez, J. Kusmierczyk-Michulec and R. Decae (2002c). Retreival of aerosol properties on regional and global scales from satellites, WMO-GAW, Riga, May 2002
- Dentener, F., J. Feichter and A. Jeuken: Simulation of the transport of Rn222 using on-line and off-line global models at different horizontal resolutions: a detailed comparison with measurements. Tellus, 51B, 573-602 (1999).
- Dubovik, O., B. N. Holben, T. F. Eck, A. Smirnov, Y. J. Kaufman, M. D. King, D. Tanre, and I. Slutsker: Variability of absorption and optical properties of key aerosol types observed in worldwide locations. J. Atmos. Sci. 59, 590-608 (2002).
- Flowerdew R. J., and J. D. Haigh: An approximation to improve accuracy in the derivation of surface reflectances from multi-look satellite radiometers. Geophys. Res. Lett. 23, 1693-1696 (1995).
- Ganzeveld, L., and J. Lelieveld: Dry deposition parameterization in a chemistry general circulation model and its influence on the distribution of reactive trace gases. J. Geophys. Res. 100, 20999-21012 (1995).
- Ganzeveld, L., J. Lelieveld, and G-J., Roelofs: A dry deposition parametrization for sulfur oxides in a chemistry and general circulation model. J.Geophys. Res. 103, 5679-5694 (1998).
- Gosse S.F., M. Wang, D. Labrie, and P. Chylek: Imaginary part of the refreactive index of sulfates nitrates in the 0.7-2.6 micron spectral region. Appl. Opt. 36, 3622-3624 (1997).
- Guelle, W., Y.J. Balkanski, J.E. Dibb, M. Schulz, and F. Dulac: Wet deposition in a global size-dependent aerosol transport model: 2. influence fo the scavenging scheme on <sup>210</sup>Pb vertical profiles, surface concentrations and deposition. J.Geophys. Res. 103, 11429-11445 (1997).
- Haywood, J.M., and O. Boucher: Estimates of the direct and indirect radiative forcing due to tropospheric aerosols: A Review. Rev. Geophys., 38,4, 513-543, 2000.
- Haywood, J.M., and V. Ramaswamy: Global sensitivity studies of the direct radiative forcing due to anthropogenic sulfate and black carbon aerosols. J. Geophys. Res. 103, 6043-6058 (1998).
- Hegg, D.A., J. Livingston, P.V. Hobbs, T. Novakov, and P.Russell: Chemical apportionment of aerosol column optical depth off the mid-Atlantic coast of the United States. J.Geophys.Res. 102, 25293-25303 (1997).
- Heimann M.: The global atmospheric tracer model tm2: Technical Report 10, Deutches Klima Rechenzentrum, Modellbetreuungsgruppe, Hamburg (1995).
- Hess M., P. Koepke and I. Schult: Optical properties of aerosols and clouds: The software package OPAC, Bull. Am. Meteor. Soc. 79, 831-844 (1998).

- Holben B. N., T. F. Eck, I. Slutsker, D. Tanre, J. P. Buis, A. Setzer, E. Vermote, J. A. Reagan, Y. J. Kaufman, T. Nakajima, F. Lavenu, I. Jankowiak, and A. Smirnov: AERONET- A Federated Instrument Network and Data Archive for Aerosol Characterisation, Rem. Sens. of the Env. 66, 1-16 (1998).
- Houweling, S., F. Dentener, and J. Lelieveld, The impact of non-methane hydrocarbon compounds on tropospheric photo-chemistry. J. Geophys. Res. 103, 10673 (1998).
- Hsu, N. C, J.R. Herman, O. Torres; B.N. Holben, D. Tanre, T. F. Eck; A. Smirnov, B. Chatenet, and F. Lavenu.: Comparisons of the TOMS aerosol index with Sun-photometer aerosol optical thickness: Results and applications. J. Geophys. Res. 104, 6269-6280 (1999).
- IPCC-TAR, Intergovernmental Panel on Climate Change Third Assessment Report, Contribution of working group I, "Climate Change 2001, The scientific basis" (2001).
- Jeuken, A.B.M., H.J. Eskes, P.F.J. van Velthoven, and E.V. Holm: Assimilation of total ozone satellite measurements in a three-dimensional tracer transport model. J.Geophys.Res. 104, 5551-5563 (1999).
- Jeuken, A.B.M.: Evaluation of chemistry and climate models using measurements and data assimilation. Ph.D. Thesis, Technical University of Eindhoven (2000).
- Jeuken, A.B.M., J.P. Veefkind, F. Dentener, S. Metzger, and Robles Gonzalez: Simulation of the aerosol optical depth over Europe for August 1997, and a comparison with observations. J. Geophys. Res. 106, 28,295-28,311. (2001).
- Kiehl, J.T., T.L. Schneider, P.J. Rasch, and M.C. Barth: Radiative forcing due to sulfate aerosols from simulations with the National Center for Atmospheric Research Community Climate Model, version 3. J. Geophys. Res. 105, 1441-1457 (2002).
- Koelemeijer R., and P. Stammes: Validation of Global Ozone Monitoring Experiment cloud fractions relevant for accurate ozone column retrieval. J. Geophys. Res. 104, 18,801-18,814 (1999).
- Liousse, C., J.E. Penner, C. Chuang, J.J. Walton, H. Eddleman, and H. Cachier: A global three-dimensional model study of carbonaceous aerosols. J. Geophys. Res. 101, 19411-19432 (1996).
- Novakov, T. and C.E. Corrigan: Cloud condensation nucleus activity of the organic component of biomass smoke particles. Geophys. Res. Lett. 23, 2141-2144 (1996).
- Meijer, E.W., P.F.J. van Velthoven, A.M. Thompson, L. Pfister, H. Schlager, P. Schulte and H. Kelder: Model calculations of the impact of NOx from air traffic, lightning, and surface emissions, compared with measurements. J.Geophys.Res 105, 3833-3850 (2000).
- Palmer, K.F. and D. Williams: Optical constants of sulfuric acid: applications to the clouds of Venus. Appl. Opt. 14, 208-219 (1975).
- Penner, J.E.: Carbonaceous aerosols influencing atmospheric radiation: black and organic carbon, in Aerosol Forcing and Climate, ed. R.J. Charlson and J. Heintzenberg, John Wiley and Sons, Chichester, 91-108 (1995)
- Quijano A. L., I. N. Sokolik, and O. B. Toon. Influence of the aerosol vertical distribution on the retrieval of the aerosol optical depth from satellite radiance measurements, Geophys. Res. Lett. 27, 3457-3460 (2000).
- Quinn P. K., D. J. Coffman, T. S. Bates, T. L. Miller, J. E. Johnson, E. J. Welton, C. Neususs, M. Miller, and P. J. Sheridan: Aerosol optical properties during INDOEX 1999: means, variability and controlling factors. J. Geophys. Res., in press (2002).
- Rajeev K., and V. Ramanathan: Direct observations of clear-sky aerosol radiative forcing from space during the Indian Ocean Experiment. J. Geophys. Res. 106, 17221-17235 (2001).
- Ramanathan, V., P.J. Crutzen, J. Lelieveld, A.P. Mitra, D. Althausen, J. Anderson, M.O. Andreae, W. Cantrell, G.R. Cass, C.E. Chung, A.D. Clarke, J.A. Coakley, W.D. Collins, W.C. Conant, F. Dulac, J. Heintzenberg, A.J. Heymsfield, B. Holben, S. Howell, J. Knudson, A. Jayaraman, J.T. Kiehl, T.N. Krishnamurti, D. Lubin, G. McFarquhar, T.Novakov, J.A. Ogren, I.A. Podgorny, K. Prather, K. Priestley, J.M. Prospero, P.K. Quinn, K. Rajeev, P. Rasch, S. Rupert, S. Sadourny, S.K. Satheesh, G.E. Shaw, P. Sheridan, and F.P.J. Valero: Indian Ocean Experiment: An integrated analysis of the climateforcing and effects of the great Indo-Asian haze. J. Geophys.Res 106, 28371-28398 (2001).
- Rasch, P.J., H. Feichter, K. Law, N. Mahowald, J. Penner, D. Benkovitz, C. Genthon, C. Giannakopoulos, P. Kasibhatla, D. Koch, H. Levy, T. Maki, M. Prather, D.L. Roberts, G.-J. Roelofs, D. Stevenson, Z. Stockwell, S. Taguchi, M. Kritz, M. Chippperfield, D. Baldocchi, P. McMurry, L. Barry, Y. Balkansi, R. Chatfield, E. Kjellstrom, M. Lawrence, H.N. Lee, J. Lelieveld, K.J. Noone, J. Seinfeld, G. Stenchikov, S. Schwartz, C. Walcek, D. Williamson: A comparison of scavenging and deposition processes in global models. Results from the WCRP Cambridge workshop of 1995. Tellus 52, 1025-1056 (2000)
- Rasch, P.J., W.D. Collins, and B.E. Eaton: Understanding the Indian Ocean Experiment (INDOEX) aerosol

- distributions with aerosol assimilation. J. Geophys. Res 106, 7337-7355 (2001)
- Robles Gonzalez C., J. P. Veefkind, and G. de Leeuw: Aerosol optical depth over Europe in August 1997 derived from ATSR-2 data. Geophys. Res. Lett. 27, 955-958 (2000).
- Robles-Gonzalez, C., J.P. Veefkind and G. de Leeuw: Mean aerosol optical depth over Europe in August 1997 derived from ATSR-2 data. Geophys. Res. Lett. 27, 955-959 (2000).
- Robles-Gonzalez, C., G. de Leeuw, P.J.H. Builtjes, M. van Loon and M. Schaap: Interpretation of retrieved aerosol properties over Europe using a chemistry transport model. Submitted to J.Geophys.Res. (2001).
- Robles Gonzalez, C., G. de Leeuw, R. Decae and J. Kusmierczyk-Michulec (2002). Uisng the ATSR-2 dual view for the retrieval of aerosol properties. IWMMM-3, Third International workshop on multiangular measurements and models, Steamboat Springs, Colorado, 10-12 June 2002, p. 45.
- Roelofs, G-J, and J. Lelieveld: Distribution and budget of O3 in the troposphere calculated with a chemistry general circulation model. J. Geophys. Res. 100, 20983-20998 (1995).
- Russell G.L., and J.A. Lerner: A finite difference scheme for the tracer transport equation. J. Appl. Meteorol. 20, 1483-1498 (1981).
- Russell, P.B., P.V. Hobbs, and L.L. Stowe: Aerosol properties and radiative effects in the United States East Coast haze plume: An overview of the Tropospheric Aerosol Radiative Forcing Observational Experiment (TARFOX). J.Geophys.Res. 104, 2213-2222 (1999).
- Seinfeld, J. H., and S.N. Pandis: Atmospheric chemistry and physics: from air pollution to Climate Change. John Wiley & Sons, Inc., New York (1998)
- Sokolik I. N., O. B. Toon, R. W. Bergstrom: Modeling the radiative characteristics of airborne mineral aerosols at infrared wavelengths. J. Geophys. Res. 103, 8813-8826 (1998).
- Stammes P., J. F. Bosma, and J. W. Hovenier: The adding method for multiple scattering calculations of polarised light. Astron. Astrophys. 225, 239-259 (1989).
- Tegen, I., P. Hollrig, M.Chin, I. Fung, D. Jacob, J. Penner, Contribution of different aerosol species to the global aerosol extinction optical thisckness: Estimates from model results. J. Geophys. Res. 102, 23,895-23,915 (1997).
- United Nations: The United Nations energy statistics database (1991). Tech. Rep. Stat. Div., New York (1993).
- Van Velthoven, P.F.J., and H. Kelder: Estimates of stratosphere-troposphere exchange: Sensitivity to model formulation and horizontal resolution. J. Geophys. Res. 101, 1429-1434 (1996).
- Veefkind J. P., G. de Leeuw, and P. A. Durkee: Retrieval of Aerosol Optical Depth over Land using two angle view Satellite Radiometry during TARFOX. Geophys. Res. Lett. 25, 3135-3138 (1998).
- Veefkind J. P. and G. de Leeuw: A new algorithm to determine the spectral aerosol optical depth from satellite radiometer measurements, J. Aerosol Sci. 29, 1237-1248 (1998).
- Veefkind J. P., G. de Leeuw, P. Stammes, and R. B. A. Koelemeijer: Regional Distribution of Aerosol over land derived from ATSR-2 and GOME. Rem. Sens. of the Env. 74, 377-386 (2000).
- Verver, G.H.L., F. Raes, D. Vogelezang, and D. Johnson: The 2<sup>nd</sup> aerosol characterisation experiment (ACE-2): Meteorological and chemical context. Tellus 52B, 126-140 (2000).
- Verver, G.H.L., D.R. Sikka, J.M. Lobert, G. Stossmeister and M. Zachariasse: Overview of the meteorological conditions and atmospheric transport processes during INDOEX 1999. J. Geophys. Res. 106, 28,399-28,414 (2001).
- Verver, G.H.L., B. Henzing, C. Robles Gonzalez: (2002). Assimilation of Aerosol Optical Depth, EGS, Nice, April 2002.

# The Advisary Group

### Members:

Dr. H. Ten Brink, ECN Prof. Dr. P. Builtjes, TNO

Dr. H. van der Woerd, Vrije Universiteit Amsterdam

Dr. H. Slaper, RIVM

# 7 Acronyms

ACE Aerosol Characterisation experiment ACTM Aerosol Chemistry Transport Model

AOD Aerosol Optical Depth

ARIA Aerosol RetrIeval and Assimilation ATSR Along Track Scanning Radiometer

AVHRR Advanced Very High Resolution Radiometer

CBM Carbon Bond Mechanism

ECMWF European Centre for Medium range Weather Forecasts

GOME Global Ozone Monitoring Experiment

INDOEX Indian Ocean Experiment

IPCC Intergovernmental Panel on Climate Change

IR Infra-Red

KCO Kaashidhoo Climate Observatory (Maldives)
KNMI Koninklijk Nederlands Meteorologisch Instituut

LUT Look-Up Table

MISR Multi-Angle Imaging SpectroRadiometer
MODIS MOderate Resolution Imaging Spectrometer

NOP Nationaal OnderzoeksProgramma luchtverontreiniging en klimaat

OMI Ozone Monitoring Instrument

POLDER Polarisation and Directionality of Earth Reflectances

SCIAMACHY Scanning Imaging Absorption Spectrometer for Atmospheric Cartography

TAR Third Assessment Report (of IPCC)

TARFOX Tropospheric Aerosol Radiative Forcing Observational experiment

TNO-FEL Fysisch Elektronisch Laboratorium

TOA Top Of Atmosphere

TOMS Total Ozone Mapping Spectrometer

TM3 Transport Model versie 3

UV Ultraviolet

WCRP World Climate Research Program

